LOCATION OF THE HIP JOINT CENTRE USING ULTRASONIC TECHNIQUES

BY

EZE SOLOMON CHIKA (B. ENG.)

This thesis is submitted in partial fulfilment of the requirements for the degree of M.Sc. in Biomedical Engineering

13th August 2015

Bioengineering Unit
University of Strathclyde
Glasgow
United Kingdom

This thesis is the result of the author's original research. It has been composed by the author and has not been previously submitted for examination which has led to the award of a degree.'

Signed: ……………………………

Date:……………………………….

ACKNOWLEDGEMENT

I would like to express my deep appreciation to my project supervisor, Mr Stephanos Solomonidis for his unparalleled support. He was always available to provide technical inputs, advice and all the material requirements that made this research work a success.

I would also like to thank in a very special way, Professor George Corner who was my co-supervisor. He made me understand ultrasound imaging techniques. His advice and motivation were remarkable.

My thanks also go to Mr Xiaowei for introducing me to the art of making tissue phantoms.

Finally, I wish to commend with my warmest gratitude, Dr Augustine Eze and my family for making this research possible.

ABSTRACT

Kinematic and kinetic gait parameters are essential indicators of musculoskeletal wellbeing. In order to accurately determine these parameters, the hip joint centre (HJC) must first be located. The accuracy with which it is located directly affects the estimated magnitude of these parameters; yet current techniques still give inaccurate results.

This study was therefore aimed at exploring the features of modern ultrasonography with a view to developing an accurate and convenient method of locating the HJC using medical ultrasound imaging.

Five participants whose BMI were less than 26.5 took part in the study in accordance with ethical approval. Ultrasound images of their hip joint were taken. Points created on the femoral head arc projected in the ultrasound image were used to fit a circle along in the probe reference frame. Coordinate transformations were then performed to relate the centre of this circle (which ought to coincide with the HJC) in pelvic anatomical reference frame.

Results obtained for one of the participants were validated with MRI technique. With respect to the position of the HJC determined from the MRI images, the ultrasound technique located the HJC to within 1mm and 3.97mm in the anterior-posterior and medio-lateral directions respectively. The inferior-superior coordinates were 41.55mm apart. Further studies are however required to refine the methodology and ascertain its accuracy limits.

TABLE OF CONTENTS

CHAPTER 1. INTRODUCTION **1**

1.1 Background 1

1..2 Aims 4

CHAPTER 2. LITERATURE REVIEW **5**

2.1 Brief anatomy of the hip joint 5

2.2 Geometry of the femur 8

2.3 Significance of the hip Joint centre (HJC) 10

2.4 Ultrasound imaging 10

2.4.1 The medical ultrasound transducer 11

2.5 Interaction of the body with ultrasound 13

2.5.1 Reflection of Ultrasound 13

2.5.2 Ultrasound Absorption 16

2.5.3 Strengths and weaknesses of medical diagnostic ultrasound 17

2.6 Ultrasonography of bone 18

2.7 Current techniques used in locating the hip joint centre 19

2.7.1 Prediction techniques 19

2.7.2 Functional techniques of locating the hip joint centre 24

2.8 Validation techniques 27

2.9 Previous studies involving the use of ultrasound in determining the HJC 28

2.10 Visit of the University of Dundee 31

2.11 Chapter summary 33

CHAPTER 3. MATERIALS AND METHODS **34**

3.1 Background 34

3.2 Equipment 34

3.3 Experimental design 36

3.4 Ultrasound data collection 39
3.5 Data collection for the functional technique 40
3.6 Algorithm development for the ultrasound method 41
3.7 Coordinate transformations for the ultrasound technique 47

CHAPTER 4. RESULTS 52
4.1 Results from the ultrasound technique 52
4.2 Results from the functional technique 52
4.3 Results from the predictive technique 54

CHAPTER 5. DISCUSSIONS 56

CHAPTER 6. CONCLUSION 61

CHAPTER 7 RECOMMENDATIONS 63
7.1 Special wears for subjects 63
7.2 Special platform on which subjects can lie supine 63
REFERENCES 64
APPENDIX A 68
APPENDIX B 71
APPENDIX C 73
APPENDIX D 75

CHAPTER 1: INTRODUCTION

1.1 BACKGROUND

The hip joint centre (HJC) is an important biomechanical consideration in gait analysis which is becoming increasingly popular as a tool for clinical rehabilitation. Gait analysis is highly relevant in the assessment of pathological conditions associated with gait and can be used to estimate musculo-skeletal loading during various activities such as sit to stand, walking and running. Suitable examples of loading variables estimated by gait analysis include force-and muscle-generating capacity of muscles, hip and knee joint moments and hip contact forces. Gait analysis can also be effectively applied to the evaluation of the outcome of clinical interventions such as total or partial joint arthroplasty which usually cause complications that can affect the gait patterns of the individuals. These benefits of gait analysis depend on the accuracy with which kinetic and kinematic data are evaluated.

The HJC is a very important factor in biomechanical calculations because it is used to define the anatomical frame of the femur (Camomilla et al., 2006). The accuracy with which it is determined also has a large bearing on the credibility gait analysis results. Errors associated with its determination are both escalated and propagated to the biomechanical data obtained for the distal part of the lower limb during gait test (Stagni et al., 2000). These errors corrupt the values of forces, moments and kinematic quantities calculated for the knee and hip joints and threaten the validity of recommendations made based on results of gait analysis. Errors during a gait test may arise from:

a. Inaccurate location of anatomical landmarks such as the anterio-superior iliac spines (ASIS) and posterior-superior iliac spine (PSIS). Locating these landmarks requires a lot of operator experience.
b. Soft tissue artifacts (STA). Gait analysis often studies the kinematics and kinetics of muscular loading. This is however achieved through markers placed over the skin. In many situations, the skin moves relative to the bone implying that

variables measured do not closely match those of the underlying skeleton. STA errors are often dependent on body mass index (BMI). This causes discrimination in the suitability of subjects for gait analysis.

c. Definition of joint centres. Human joints are very irregular and often do not have a simple geometrical centre. Defining the joint centre therefore requires skills. For example, the knee joint centre is usually determined by locating the lateral epicondyle of the femur by palpation. Half of the measured knee width is then added medially to determine the position of the knee joint centre. The accuracy of this technique often depends on the precision with which the lateral epicondyle of the femur is located. However, locating the epicondyle precisely always requires skill and the difficulty in locating the knee joint centre does not compare to that of locating the HJC. This is because the HJC is more deeply situated beneath the tissues and covered by many ligaments, tendons and muscles.

Several approaches of locating the position of the HJC in 3D space have been developed. These are traditionally classified as predictive and functional. The predictive techniques are derived from regression equations relating the HJC to the spatial relationships among special anatomical land marks of the pelvis and lower limb. These equations were formulated either after radiographic study of the pelvis and lower limb anatomy (Bell et al., 1990; Davis etal.,1991; Harrington et al., 2007) or by physical study of the human cadaver (Seidel et al., 1995). The regression equations developed by Davis et al (1991) has the greatest popularity and commercial use and are used in the VICON plug in gait model (Plug in gait manual).

The functional techniques were developed to offer more accurate subject dependent HJC coordinates. To use a functional technique, markers are attached to the thigh and pelvis. Those attached to the pelvis are used to locate its anatomical landmarks. The limb is then moved in prescribed pattern while the trajectory of each marker is recorded by a motion capture system. A suitable algorithm based on either geometric sphere fitting (e.g Sphere fitting algorithm by Pratt), least squares sphere fitting (eg, by Gamage and Lasenby, 2002) or coordinate transformation (eg. Centre transformation technique CTT or Symmetrical centre of rotation estimate, SCoRE) is then used to locate the HJC based on the collected data. Although there is usually no general consensus about the better of the two techniques, the Harrington's (Harrington et al., 2007) prediction equations are highly recommended by the international society of biomechanics (ISB) while the geometric sphere fitting algorithm is recommended as the best for the functional techniques (Kainz et al., 2015). Additionally, the society recommends that functional techniques should be used on subjects that have substantial range of motion at the hip while the Harrington's technique should only be used when the subjects cannot move their lower limbs in sufficient hip range of motion. This presents the functional technique as the first choice method and highlights the importance of hip range of motion to its success.

Results obtained from the two methods are usually validated using MRI, X-Ray and CT imaging modalities. These modalities are known to give accurate results since the whole of the joint and the anthropometric landmarks become visible, allowing the HJC to be located by simple measurements. Validation techniques are essentially limited to being used as gold standard in validating other techniques. This is due to the high cost of acquiring MRI and CT equipment and radiation invasiveness of X –ray.

The application of ultrasound to HJC determination is an emerging trend brought about by the increasing sophistication in the capabilities of commercial medical ultrasound equipment. Ultrasound techniques of locating HJC would offer a non-invasive, cost effective, convenient and subject-specific alternative to existing methods. It will also eliminate the rigors of moving the limb in predetermined patterns as demanded in functional methods. The technique can therefore be applied to any subject no matter the age or health status. However, the exact methodologies of using this technique is not often stated clearly in literature; even by authors that claimed to have used them as gold standard.

1.2 AIMS

In view of the foregoing, this study aims to:

Study the improvements accompanying the Analogic Ultrasonix Q+ equipment recently acquired by the department of Biomedical Engineering of the University of Strathclyde with a view to using all the features effectively in creating musculo-skeletal ultrasound images.

a. Critically study existing techniques of determining the HJC. This knowledge base will be relevant to comparing or validating results of current study.
b. Develop a simplified technique of locating the hip joint centre in 3D space both by performing ultrasound imaging of the hip joint and by using existing data on the geometry of the human femur and pelvis.
c. To perform a functional technique of HJC determination.
d. To locate the HJC using the predictive technique
e. To compare results of the ultrasonic technique with those of the functional and predictive techniques.

CHAPTER 2: LITERATURE REVIEW

2.1 BRIEF ANATOMY OF THE HIP JOINT

The hip joint, referred to as the *acetabulofemora*l joint is one of the most important load-bearing joints in vertebras. The joint which is usually classed as ball and socket, articulates the femur to the acetabulum where the pubis, ilium and ischium bones are fused together. The femur's convex hemispherical head embeds in the concave hemisphere of the acetabulum thus conferring upon the joint, a wide range of motion in the sagittal, frontal and coronal planes. Figs. 2.1a and 2b present the anatomy of the hip joint.

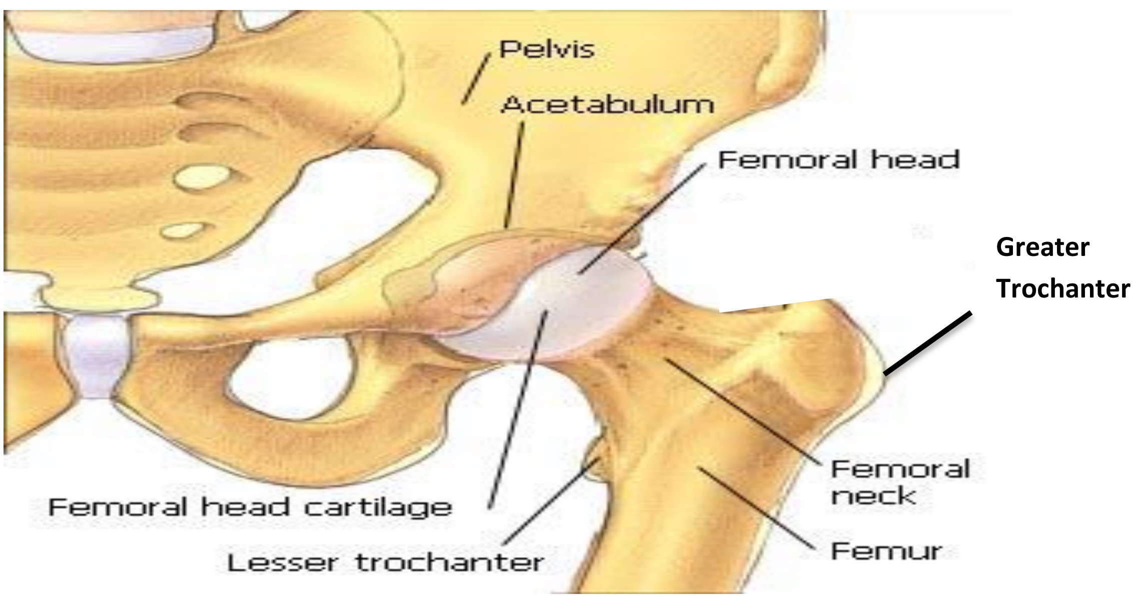

Figure 2.1a: Anatomy of the hip joint showing the femoral head as approximating a hemispherical shape which is embedded in the acetabulum. Image taken from (http://www.rudyard.org/hip-joint-anatomy/)

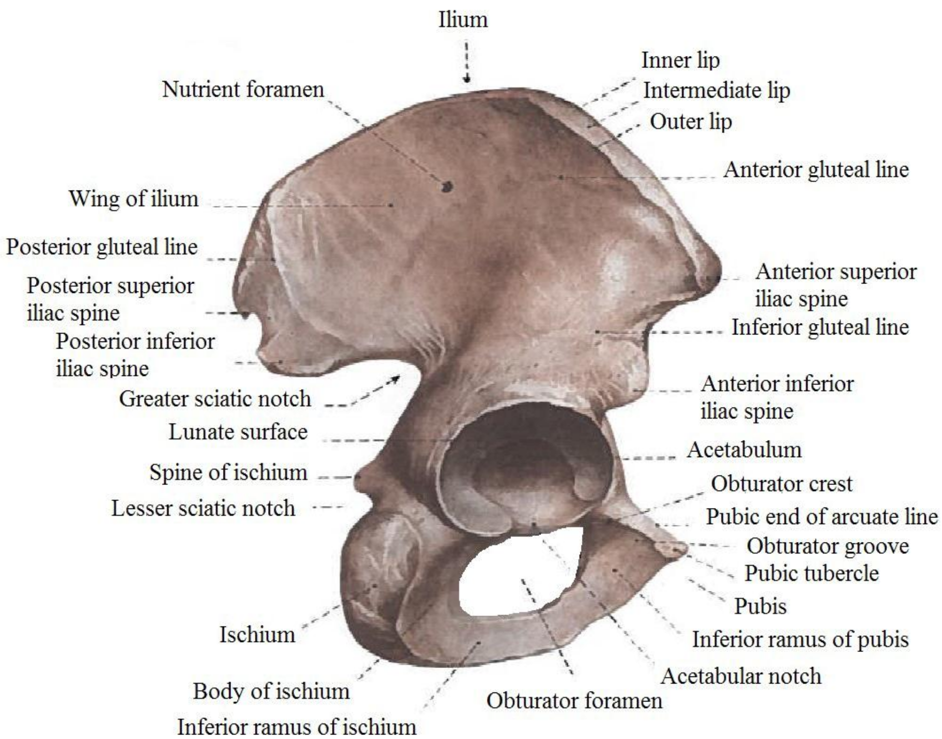

Figure 2.2b: Bones of the acetabulum. Image also shows the hemispherical concave of the acetabulum. (http://www.rudyard.org/hip-joint-anatomy/)

The femoral head is attached to the acetabulum by three main ligaments:

a. the iliofemoral ligament which attaches the ilium to the femur at the greater and lesser trochanter,

b. the ischiofemoral ligament which links the acetabulum to the greater trochanter and

c. the pubofemoral ligament which attaches the lesser trochanter to the superior ramus of the pubic bone just superior to the obturator foramen.

The acetabular labrum which is a fibrous cartilage ring surrounding the acetabulum ensures the stability of the embedded femoral head by deepening the acetabulum.

The structure of the joint, cartilages, tendons and muscles equip the hip joint sufficiently to support flexion/extension, abduction/adduction and circumduction. The muscles of the hip are usually categorised into flexors, extensors, abductors and adductors. Flexor group of muscles are anterior to the hip and comprise of Quadriceps Femoris and Ilio-Psoas muscles. The Quadriceps Femoris is made up of four distinct muscles: Vastus Medialis, Vastus Intermedius, Vastus Lateralis and Rectus Femoris. The Ilio-Psoas muscle is also made up of the Psoas major and the Iliacus muscle. This group of muscles constitutes about 70% of the thigh's total mass and control the flexion of the hip.

The adductor muscles of the hip include Adductor Longus, Adductor Brevis, Adductor Magnus, Gracilis and Pectineus muscles. This group of muscles is associated with hip adduction. Figure 2.3 shows the hip joint covered by muscles and tissues.

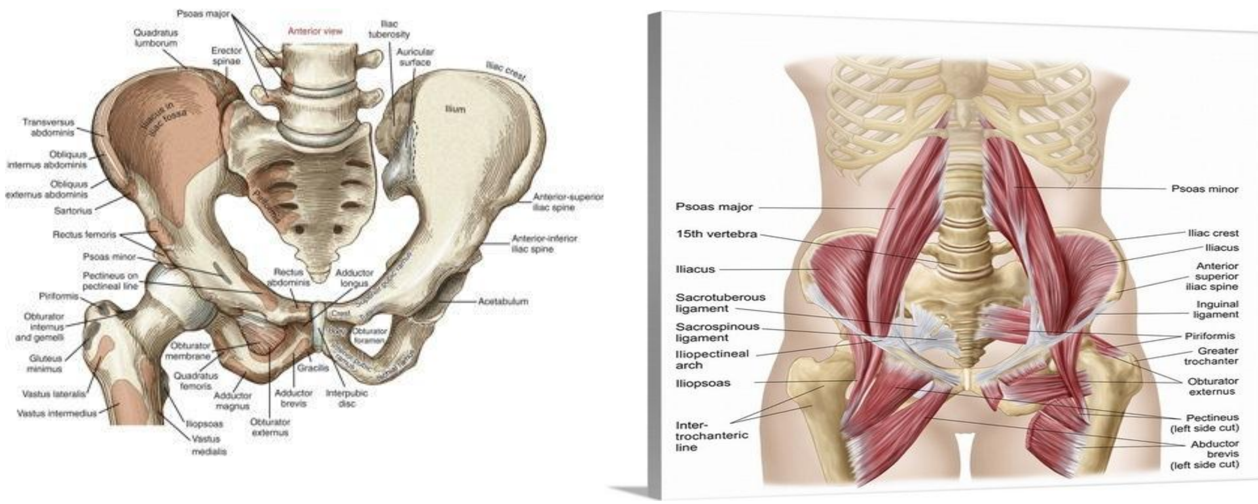

Figure 2.3: Images showing the hip joint and how it is covered by muscles and tissues (https:// http://free-stock-illustration.com/hip+muscles+anatomy?image=1262775607)

Abductors of the hip include the Sartorius and the Gluteus Medius and minimus while extensors are the gluteus maximus and hamstring muscles. The hamstring muscles are made up of the Biceps Femoris, Semi-Membranosus and Semi-Tendinosus muscles.

2.2 GEOMETRY OF THE FEMUR

The HJC in a normal hip is coincident with the centre of the acetabulum in which the femoral head is located. The articular portion of the femoral head forms two-thirds of a sphere, having a flat surface at its upper part. There is also a central depression on the medial surface called Fovea Capitis Femoris, and this gives insertion to the ligament of the femoral head.

The femoral neck supports and joins the head to the shaft. Its axis is oblique in nature and is situated superiorly, medially and anteriorly with respect to the shaft of the femur. It makes an angle known as the neck angle in the frontal plane. The magnitude of this angle in adults is about 130 degrees. In the transverse plane, it subtends an acute angle known as the anteversion that has an average value 7.5 degrees for adults. Figure 2.4 and table 2.1 summarise these details which were originated from Yoshioka Y., Siu D., and Cooke T.D.V. (1987). The authors derived their data after studying the geometry of the femoral anatomy using thirty two cadaveric femurs obtained from the Anatomy department of Queen's Land University Ontario, Canada. Similarly, RC Siwach & S. Dahiya (2003) found from their own study that anthropometric features of the human femur vary in size across races.

Serial	Parameter	Females	Males
1.	Femoral head diameter(mm)	45 ± 3.0	52 ± 3.3
2.	Neck shaft angle (deg)	133 ± 6.6	129±7.3
3.	Anteversion (deg)	8 ± 10	7.0 ± 6.8

Table 2.1: Geometry of the proximal Femur showing the femoral head diameter, neck shaft and anteversion angles data (±S.D). Yoshioka Y., Siu D., and Cooke T.D.V.(1987).

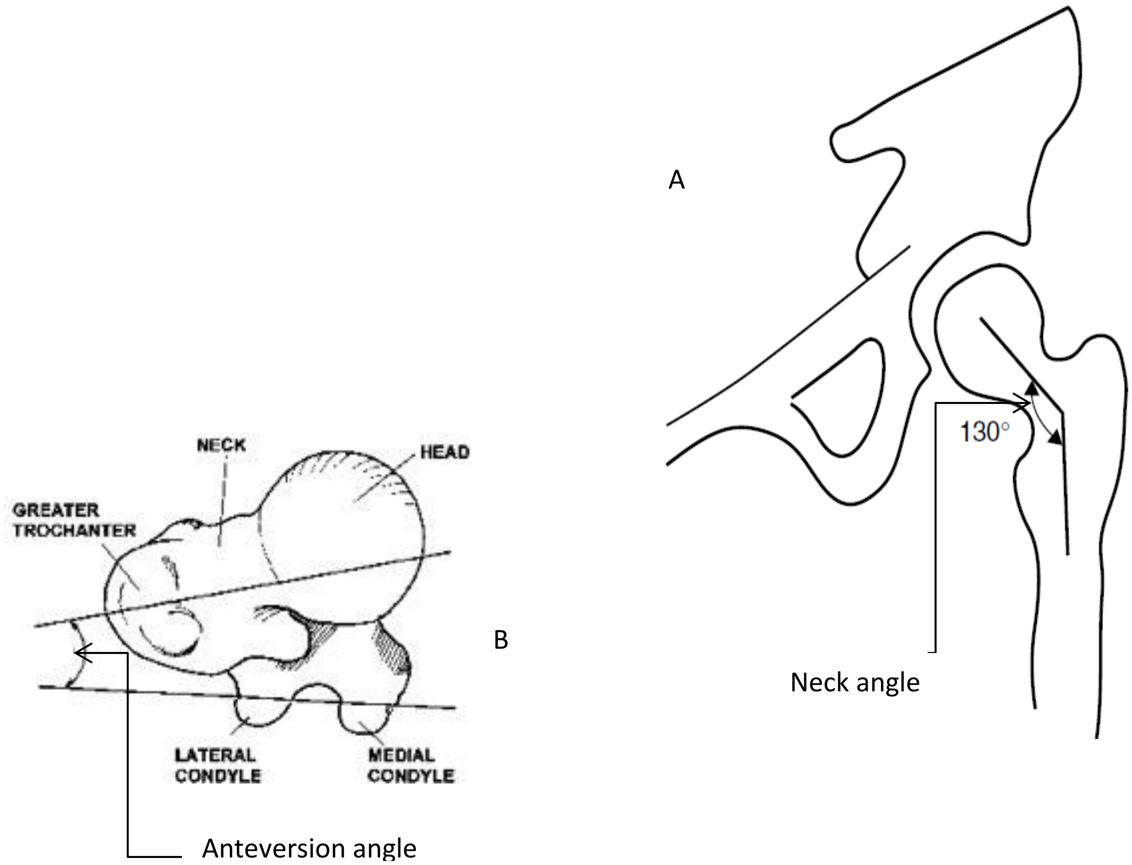

Fig 2.4: The human femur: Image A shows the neck angle (frontal view of the femur) while B shows the anteversion angle (transverse view of the femur). Yoshioka Y., Siu D., and Cooke T.D.V.(1987).

Menschik, (1997) observed that the shape of the hip joint is more appropriately described as conchoid. This according to (Kang et al, 2009), implies that accurate location of the HJC cannot be determined using ordinary techniques. This is because conchoids do not have equal axes. However, most HJC estimation techniques approximate the joint as a sphere and several optimization procedures have been implemented to drastically reduce errors.

2.3 SIGNIFICANCE OF THE HIP JOINT CENTRE (HJC)

Biomechanical analysis of gait gives insight into the magnitude, direction and sense of forces and moments acting on human joints. Nowadays, gait analysis also finds increased medical relevance. Locating the hip joint centre accurately is a critical requirement to the validity and reliability of recommendations derived from the analysis. In the post-operative rehabilitation of prosthetic patients, accurate location of hip joint centre is necessary to quantify the musculoskeletal loading of the hip joint. The task is somewhat more challenging with pathologic subjects whose hip orientation and symmetry may have been altered. In all cases however, locating the hip joint centre incorrectly leads to error in the calculated hip joint reaction forces, torque and power (Ehrig et al., (2011), Kainz et al., (2004) and Bouffard et al., (2012). It is therefore pertinent to develop a method that can give the centre of the hip joint with as minimal error as possible.

2.4 ULTRASOUND IMAGING

Ultrasound is an acoustic pressure wave beyond human audible range (frequency is above 20 kHz). It is commonly generated by a piezoelectric transducer. Piezoelectric materials are made up of crystals which vibrate when connected to electric voltage source due to rapid changes in their shapes. When mechanically vibrated, a piezoelectric material generates electrical voltage, in a phenomenon called piezoelectric effect. The process by which piezoelectric crystals vibrate to generate ultrasound is called reverse piezoelectric effect. The word ‘piezo’ is taken from the Greek word ‘piezein’ which means to squeeze or to press.

The non-ionizing nature of ultrasound imaging modality as well as its affordability contributes to its increasing preference in medical imaging and diagnosis. Musculoskeletal ultrasound imaging is consequently, becoming very popular as an alternative to X-ray and CT scan which both release ionizing radiation into the body. The determination of hip joint centre using this method is therefore expected to be more convenient, less expensive and most of all, very safe.

2.4.1 The Medical Ultrasound Transducer

A transducer is a device capable of converting energy from one form to another. The ultrasound probe is therefore a transducer which converts electrical energy of the supply voltage into mechanical (vibration) energy. The vibration generates ultrasound waves of very high frequencies. For medical diagnostic ultrasound imaging, the frequency is usually in the range of 1-30MHz (S. Lddr et al., manual of diagnostic ultrasound)

The diagnostic ultrasound transducer is constructed as laminate of thin sheets of artificial ceramic materials. A typical example of ceramic material in widespread use in this respect is lead zirconate Titanate commonly known as PZT which is also an excellent dielectric and Ferro-electric material. PZT is a solid state solution of Lead Titanate ($PbTiO_3$) and Lead Zirconate ($PbZrO_3$) which forms a perovskite crystal structure. Generally any crystal structure resembling that of calcium Titanate with oxygen atom at a face centre is referred to as a perovskite structure. The thickness of the laminate used in the ultrasound transducer determines the frequency of the generated ultrasound pulses. Figure 2.6 shows a schematic diagram of an ultrasound probe that is emitting pulses.

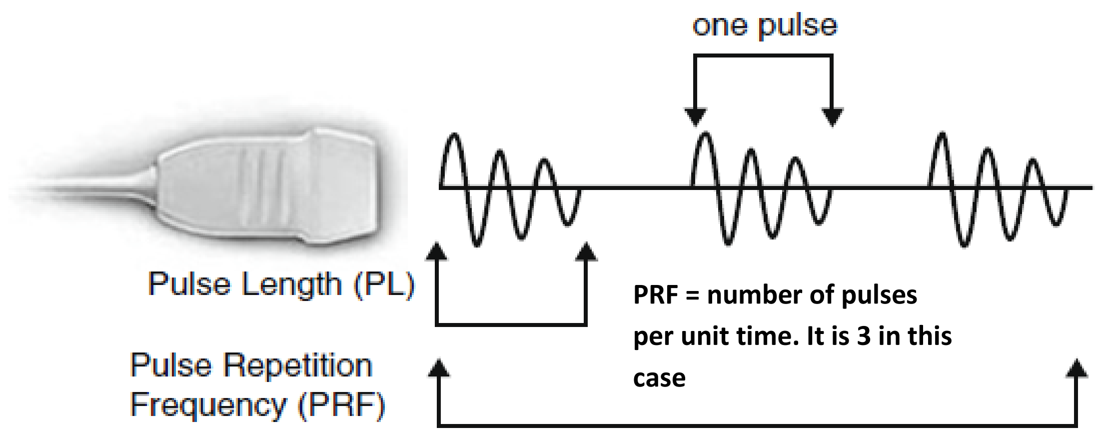

Figure 2.5: Schematic diagram of a diagnostic ultrasound transducer probe emitting pulses. The pulse repetition frequency (PRF) is the number of pulses emitted by the probe per unit time. For medical imaging devices, PRF ranges from 1-10kHz. Taken from Narouze SN., (2011).

It is worthy of note also, that a particular piezoelectric crystal in the laminate can receive signal when not emitting. Thus, the reflected fraction known as the echo is received by the transducer and the computer constructs image of the internal parts of the body based on the information contained in the echo. The depth of the boundary within the tissue or organ is calculated using the following fundamental relationship:

$$d = c \times \frac{T}{2} \quad \ldots\ldots\ldots\ldots\ldots\ldots\ldots\ldots\ldots\ldots\ldots\ldots\ldots (2.1)$$

Where c = velocity of propagation of sound in the medium

T = time taken to sense the reflected sound wave at the transducer.

Ultrasound transducer probes are usually available in various sizes and shapes. The frequency of the transmitted wave is related to the probe's size and is a measure of the depth that the ultrasound wave can penetrate in the tissue or organ. The shape on the other hand, determines its field of view known as the foot print. For any scan, the appropriate probe has to be used to ensure accuracy.

2.5 INTERACTION OF THE BODY WITH ULTRASOUND

The ultrasound used clinically interacts with the body in characteristic ways. It is reflected, refracted, absorbed and interfered. These properties are discussed briefly in the next subsections.

2.5.1 Reflection of Ultrasound

Ultrasound pulses travel into the body, strike the tissue or organ boundaries and are reflected at different rates. Two types of reflection are common with ultrasound:

a. Specular reflection
b. Scattered or non-specular reflection.

Specular reflection obeys the law of reflection. This requires the surface to be large and smooth. Such surfaces are called specular reflectors. Since the law of reflection is obeyed, the incident ultrasound beam must then subtend an angle which is equal to the angle between the echo and an imaginary line normal to the point of incidence. Hence,

Angle of incidence = Angle of reflection ………………………………………….(2.2)

The intensity of the echo is dependent on both the incident ultrasound beam and the difference in acoustic impedance (Z) of the media that form the acoustic boundary. The echo achieves the greatest intensity for a particular acoustic boundary when the angles of incidence and reflection are coincident with the imaginary normal line. This situation is shown in figure 2.7 below. Echo intensity, incident beam and acoustic impedance have a special relationship illustrated in figure 2.8 and expressed in equation 2.3.

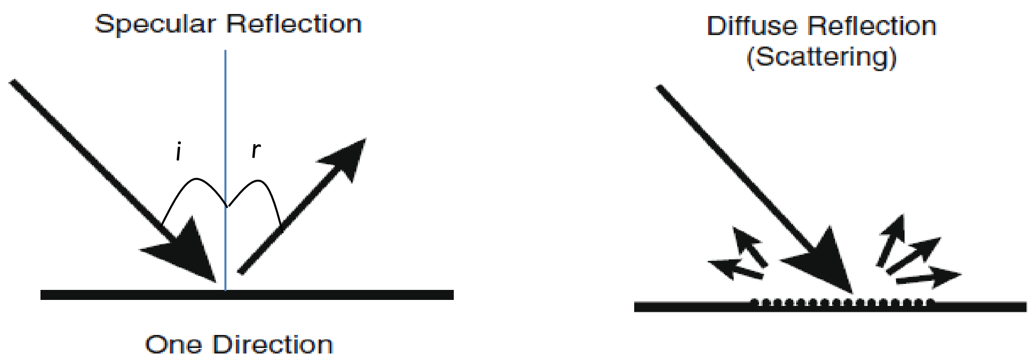

Figure 2.6: Schematic drawing showing specular and scattering reflection of ultrasound waves. In the specular reflection, i = r . (*Narouze SN.,(2011)*)

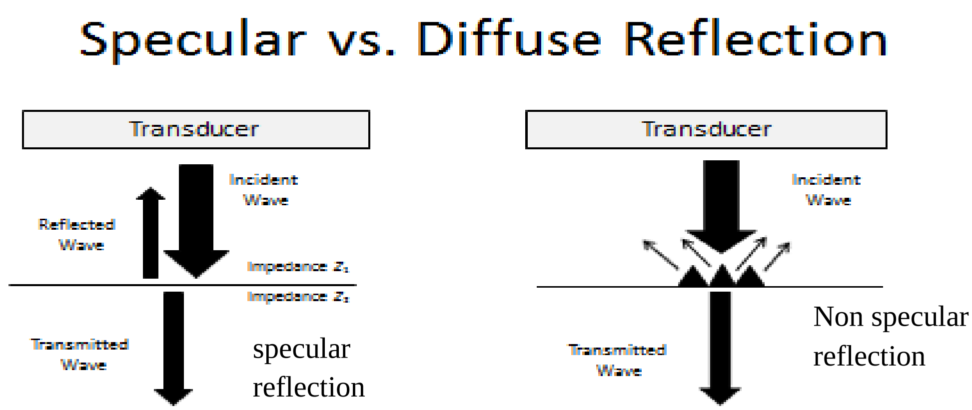

Figure 2.7: Ultrasound interaction with surfaces (Narouze SN.,(2011))

$$\frac{Ir}{Ii} = \frac{(Z1-Z2)^2}{(Z1+Z2)^2} \qquad \text{……………………………………………………………….(2.3)}$$

Where:

$Ir = Intensity\ of\ the\ echo,$

$Ii = Intensity\ of\ incident\ ultrasound$

$Z1 = Acoustic\ impedance\ of\ first\ medium,$

$Z2 = Acoustic\ impedance\ of\ the\ second\ \ medium$

The relationship shows that large acoustic differences or mismatch increases specular reflection. Table 2.2 below shows acoustic impedance values for various materials.

S/N	Body Tissue/Material	Acoustic Impedance (Rayl)
1	Air (STP)	0.0004
2	Water	1.48
3	Brain	1.58
4	Fat	1.38
5	Liver	1.65
6	Blood	1.61
7	Kidney	1.62
8	Muscle	1.7
9	Soft tissue (average)	1.63
10	Bone	7.8

Table 2.2: Showing acoustic properties of tissues and materials. Ultrasound imaging gives best results for materials with comparable acoustic impedances. Imaging involving bone and air requires acoustic matching. Data from international society of radiology (http://www.isradiology.org/isr/docs_books/basic/Chapter3.pdf)

An image obtained from ultrasound scan of a bone-soft tissue and soft tissue-gas boundaries would produce a large echo because of the large difference in the values of their acoustic impedances. This is due to high specular reflection that would result since the pairs have huge acoustic mismatch. For this reason, acoustic gel is always applied generously on the skin when conducting an ultrasound scan, to eliminate air so as to create impedance as close to that of the skin as possible. The use of a matching layer such as gel, to match acoustic impedances of two different layers is known as acoustic matching. The present study will involve a bone-tissue interface; acoustic matching will be impossible since the surface is in vivo.

Scattered or non-specular reflection is irregular and does not obey the law of reflection. It occurs when the diameter of the reflecting surface is much less than one wavelength of the ultrasound beam. Ultrasound equipment use scattered reflection to reveal meaningful details about the texture of internal organs of the body.

2.5.2 Ultrasound Absorption

Another very important property of ultrasound is absorption. This refers to the loss of the ultrasound energy to a medium. For a particular medium, absorption is proportional to the viscosity, relaxation time and ultrasound frequency. In medical imaging, absorption is also an important consideration as it continues to diminish the ultrasound energy making it difficult to reveal images of the anatomy located deep in the body. Figure 2.9 compares the absorption capabilities of various tissues.

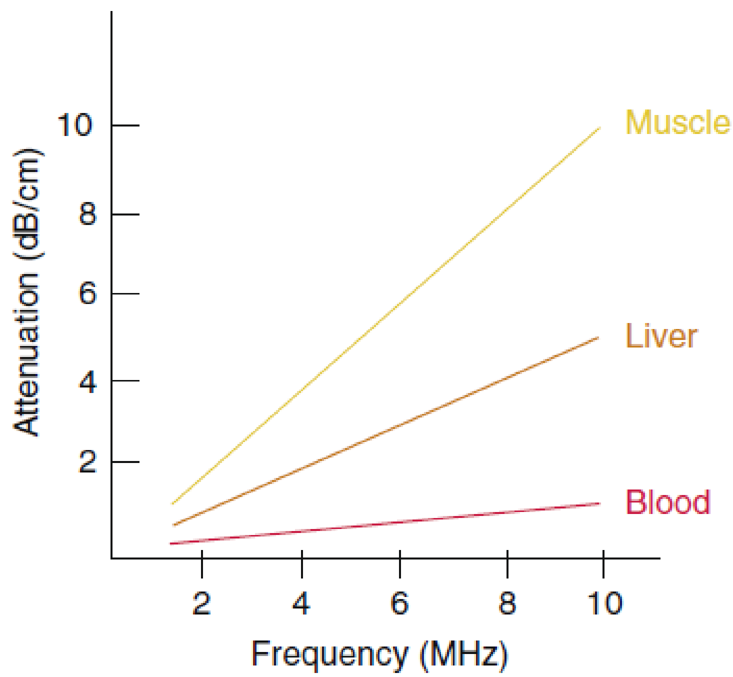

Figure 2.8: Attenuation capabilities of various tissues. At any frequency, muscles attenuate ultrasound beam the most followed by liver and then, blood. Nasrouze SN (2011)

Bones are the greatest ultrasound absorbers in the body. Thus when an ultrasound beam strikes a bone surface, it both undergoes specular reflection and massive absorption. This explains the so called acoustic shadow cast on the anatomy beneath a bone in ultrasound images. This may be a challenge to the current study. A possible solution however, would be to experiment scanning with various frequencies in order to select the range that would guarantee optimum resolution.

2.5.3 Strengths and Weaknesses of Medical Diagnostic Ultrasound

Like every other imaging modality, ultrasound has its strengths and weaknesses. It is popularly known to be the safest of all imaging systems as it does not expose patients to ionizing radiation which can cause damages (e.g cancer) to tissues. In general, the effect of ionizing radiation has not been fully understood. It is however believed to be cumulative with time, making the adoption of 'maintaining the dosage as low as reasonably achievable' (ALARA principle) highly expedient. However, ultrasound does not release any form of ionizing radiation.

Medical ultrasound does not produce any dangerous magnetic field as applicable with the magnetic resonance imaging (MRI) modality. This implies that it can be used on any patient and in any environment without fear of accidents. Ordinarily, patients with implants made of ferrous metals may cause a great risk both to themselves and to clinicians if attempt is made to scan them with the MRI. Interaction of these implants with the strong magnetic fields created by MRI equipment would cause dangerous accidents and serious injuries to patients. This may also cause 'missile effect'

Claustrophobia is an issue with the MRI and computed tomography (CT) scan. Patients often feel anxious being in the equipment gantries. This is not a problem with ultrasound equipment. Ultrasound is also superior in terms of patient comfort as they are usually examined when lying down or seated in a padded chair. The portability of ultrasound equipment is another important consideration. This makes ultrasound easy to deploy to any department or ward in the hospital where it is needed. Being portable and relatively cheap, ultrasound has the potentials of being used as a point of care device. Medical techniques based on ultrasounds therefore, also has potentials of widespread adoption.

A major short coming with ultrasound is that it does not penetrate the bone. It is thus not suitable for studying areas in the anatomical depth. This shortcoming places a limit currently, to the use of ultrasound in orthopedics. Another shortfall for ultrasound is its heavy dependence on operator expertise. It is a prerequisite for the operator to be skilled in the recognition of anatomical structures in order to acquire an image of diagnostic relevance. Any feature missed or misrepresented may give contradicting information about a pathological condition. Ultrasound is also limited in field of view as it cannot be used to view any anatomical structure beneath or behind a bone.

2.6 ULTRASONOGRAPHY OF BONE

Ultrasound is often wrongly believed to be irrelevance in orthopedics due to its inability to penetrate the bone. Generally, diagnostic frequency range used in ultrasound does not allow for bone penetration. However, the high acoustic impedance of the tissue-bone interface due to bone's hard cortical surface results in strong reflection of ultrasound wave. Due to the lack of signal beyond the cortical surface, the only thing visible is a dark homogenous region which sonographers call acoustic shadow. Due to acoustic shadowing, there is no information revealed beyond the cortical surface of bone. However, musculoskeletal ultrasound still finds growing adaptation in medicine and its use in orthopedic diagnosis has been variously reported in recent medical literature, including in the diagnosis of fractures and other orthopedic pathologies (*Role ultrasound in orthopedics, a review; 2011*).

Orthopedic ultrasound depends on the hyper echoic reflection in the cortical membrane of bones as seen in an ultrasound image (Backhaus et al. 2001). With the requisite knowledge and skills, it is possible to derive vital information from an ultrasonic bone image

2.7 CURRENT TECHNIQUES USED IN LOCATING THE HIP JOINT CENTRE

Several attempts have been made to accurately locate the centre of the hip joint. Stagni et al. (2000) highlighted the need to develop techniques for accurate determination of the HJC. They observed calculated hip flexion/extension moment was less by up to 22% when the estimated HJC was mislocated by 30mm anterior to the proper location. The authors also found that 30mm lateral error in HJC location caused a reduction by about 15% in calculated hip abduction/adduction moment.

The task of locating the HJC accurately is made very challenging by the anatomical location of the joint under the covering of thick layers of muscles and other tissues. Thick covering of the HJC by tissue implies that the use of palpation or surface estimation in finding its location accurately is difficult (Laskin, 1984). The soft tissue covering also introduces errors known as soft tissue artifact (STA). The femoral head which embeds in the bony hemispherical concave of the acetabulum also constitutes a challenge especially for techniques relying on ultrasound imaging. Despite these drawbacks, several techniques have been developed for locating the HJC in space. The methods used are classified as follows:

a. Prediction techniques
b. Functional techniques

2.7.1 Prediction Techniques

Prediction techniques of locating the hip joint centre in space refer to a collection of methods relying on established geometrical correlation among the hip joint centre and some palpable bony landmarks in the pelvic region. Andriacchi et al. (1980) and Tylkowski et al (1982) were the first to develop techniques that use palpable anatomical landmarks of the pelvis to locate the HJC. Their studies were both based on radiographs. Andriacchi’s prediction technique located the HJC at 1.5 to 2cm distal to the midpoint of the line joining the ASIS to the pubic symphysis, in the frontal plane. Their work failed to reveal how far medial from the greater trochanter the HJC was located. On the other hand, Tylkowsky et al., (1982) examined anterior-posterior and lateral pelvic X-ray images of 200 patients with various musculoskeletal impairments at the Children's Medical Centre Growth Study Clinic, Boston. They used five skeletal cadavers to estimate the location between of the hip joint centre in terms of the inter ASIS distance as follows: 12% Distal, 11% medial and 21% posterior to the ASIS. Exact methods through which these results were obtained are however, not documented. The results may also not be suitable for normal population.

Bell et al., (1989) combined the prediction methods developed by Andriacchi and Tylkowski to develop a method which locates the HJC in terms of percentages of the inter ASIS distance as follows: 30% distal, 14% medial and 22% posterior relative to ASIS of the tested side. The authors proved that the method they developed which precludes radiation exposure was better than surface estimation method used in Eberhart and Inman (1951). Laskin (1984) also demonstrated that surface estimation of the HJC gave results which were over 4cm and 2cm away from the actual position in 12% and 88% of the cases respectively.

Bell et al.,(1990) used reflective markers and photogrammetry to compare the results of Bell et al., 1989. They found the two results were similar except with 19% of inter ASIS distance posterior to ASIS against 22% obtained in the previous study. They attributed the difference to photogrammetric effect.

Seidel et al., (1995) demonstrated that the HJC location cannot be determined accurately by simply expressing it as percentages of pelvic width alone. Their study, based on 65 dissected adult human cadavers (35 female and 30 male) led to the development of two sets HJC predicting techniques, both with respect to the ASIS. The first relations are expressed in terms of the pelvic with (PW) inter ASIS span as:

14% (SD. 3%) of PW medially, 24% (SD. 3%) of PW posteriorly and 30% (SD. 4%) of PW inferiorly. This method expressed in terms of PW alone gave less accurate result than the second, which is:

14% (SD.3%) of PW medially, 34% (SD. 2%) of PW posteriorly and 79% (SD. 5%) of PH inferiorly**.**

Of all predictive methods available at the time, Leardini et al, (1999) noted that those developed by Bell et al (1990) were the most accurate equations (with errors in the range 9 - 20mm while Davis et al (1991) had the most widely used of all regression equations. The popularity of Davis' technique may be associated with the relative ease with which anthropometric data required for its estimation are gathered. Davis et al., (1991) developed predicting relationships that express the HJC in the pelvic coordinate system shown in fig 2.9 below.

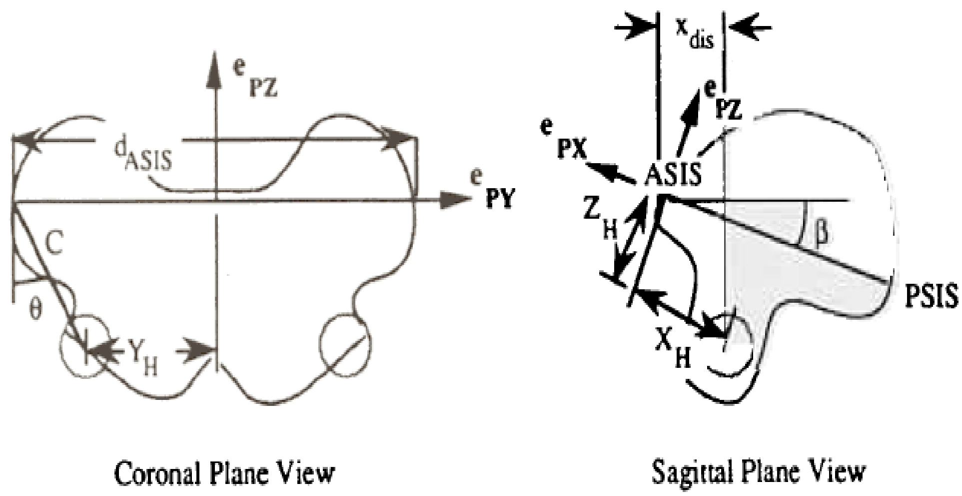

Figure 2.9: Pelvic Anatomical Landmark Frame, taken from (Davis et al., 1991).

. The relations are as follows:

X_H= -0.95D + 0.031L – 4……………………………………….(2.4)

Y_H = -0.31D – 0.096L + 13……………………………………. .(2.5)

Z_H = 0.5PW – 0.055L + 7………………………………………..(2.6)

Where X_H, Y_H, and Z_H are as above while 'L' is distance between ASIS and homolateral medial malleolus in millimeters. The authors also relied on existing correlation among various anthropometric features. The prediction equations were developed as follows

Θ and β were found to be 28±6.6 and 18±4 degrees respectively

$$C = 0.115L_{leg} - 0.0153 \quad \text{R-square correlation} = 0.9 \ldots\ldots\ldots\ldots (2.7)$$

$$X_H = [\, -x_{dis} - r_{marker}] \cos(\beta) + C \cos(\Theta) \sin(\beta), \ldots\ldots\ldots\ldots (2.8)$$

$$Y_H = S[\, C \sin(\Theta) - d_{ASIS}/2] \ldots\ldots\ldots\ldots (2.9)$$

$$Z_H = [-x_{dis} - r_{marker}] \sin(\beta) - C \cos(\Theta) \cos(\beta) \ldots\ldots\ldots\ldots (2.10)$$

Where d_{ASIS} = inter ASIS distance in meters measured during clinical examination

X_{dis} = anterior/posterior component of ASIS/ hip joint centre distance (in metres) in the sagittal plane of the pelvis measured during the clinical examination,

r_{marker} = marker radius (in metres)

S = +1 for right side and -1 for left side.

Another set of HJC prediction relationships was developed by Harrington, et al., (2007) who used broader sample comprising children, adults and patients with cerebral palsy. They reviewed the regression equations of Davis et al (199) and Bell et al (1991) to come up with theirs. Their results also compute the HJC both in terms of pelvic anatomical reference and as functions of the pelvic width and depth. This technique has been shown to be more superior to others in terms of accuracy and has been adopted by the ISB as such. The equations are:

$$X = -0.24PD - 9.9 \ldots\ldots\ldots\ldots (2.11)$$

$$Y = -0.30PW - 10.9 \ldots\ldots\ldots\ldots (2.12)$$

$$Z = 0.33PW + 7.3 \ldots\ldots\ldots\ldots (2.13)$$

X, Y and Z are consistent with the PAC system defined above.

It was earlier stated that the International society of Biomechanics (ISB) adopted the Harrington's prediction method as the most accurate. However, Anderson et al., (2015) specifically compared its accuracy with those of Davis et al (1991) and Bell et al (1989) on eighteen patients of metal-on-metal hip arthroplasty. In their results (summarized in figure 2.10) the Harrington's method gave significantly different mediolateral coordinate of the HJC. The authors also found that none of the regression methods gave sufficiently accurate results and thus, suggested the use of medical imaging modalities in situations that require the HJC to be located with high accuracy.

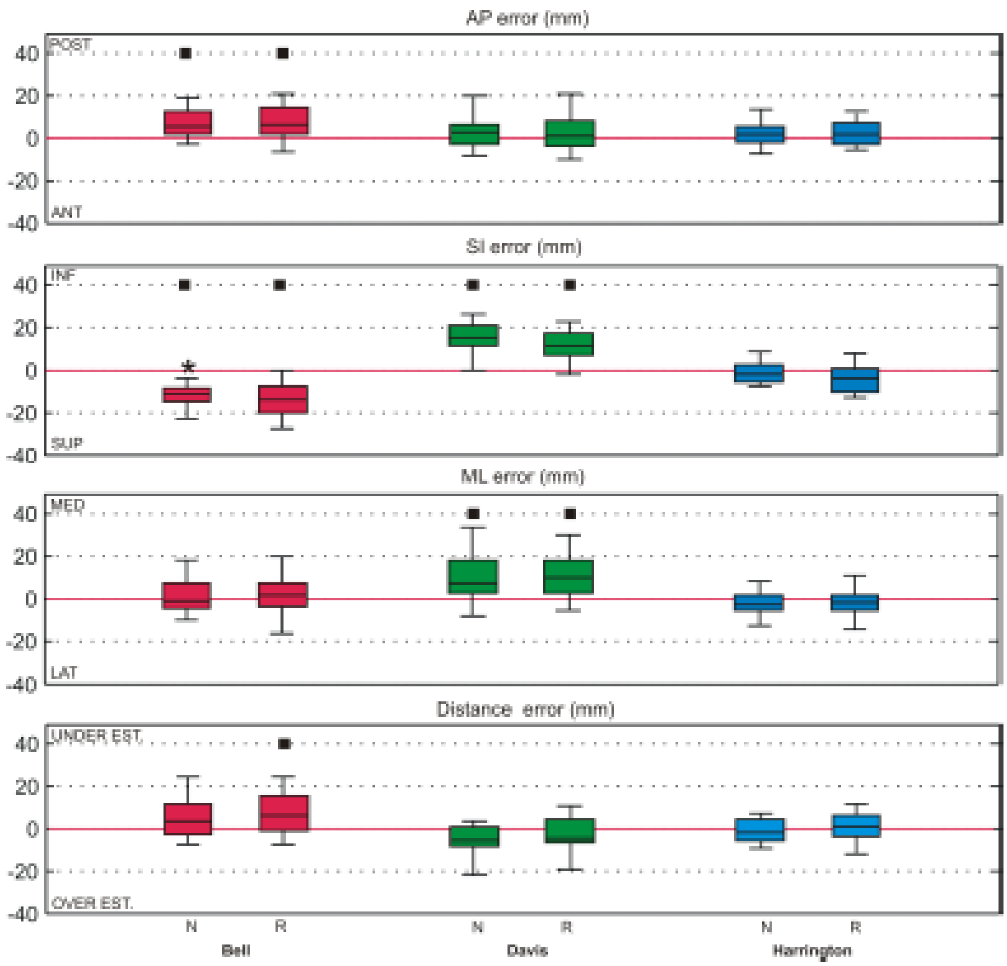

Fig. 2.10 Box and whisker plot comparing HJC calculated using regression equations proposed by Bell, Davis and Harrington.AP, SI and ML respectively refer to anterior-posterior, superior-inferior and medio-lateral directions with respect to the actual position of the HJC. 'N' stands for native hip while 'R' is for resurfaced hip. (Anderson et al., 2015)

One other form of predictive method popularly called the greater trochanter (GT) method locates the HJC at 25% of the distance between the ipsolateral and contralateral greater trochanter. O'Conor K. M and Weinhandl J. T (2014) used coefficient of multiple correlation to compare the reliability and repeatability of the GT method with the regression method of Bell (BELL) et al.,(1989). They found significant differences. Their results may be questionable since the functional technique used as gold stand in the study have great tendency to locate the HJC with errors.

2.7.2 FUNCTIONAL TECHNIQUES OF LOCATING THE HIP JOINT CENTRE

Functional techniques of locating the HJC are non-invasive methods developed to offer subject-specific results (Camomilla et al; 2006). In this technique, the HJC is calculated using photogrammetry. Reflective markers are attached at ASISs, PSISs and thigh and the leg is moved in any combination of flexion/extension, abduction/adduction and circumduction. As the subject moves the leg, installed motion camera system tracks the trajectories of the markers in space. The spatio-temporal data are then used with appropriate algorithm to locate the hip joint centre. Very substantial range of motion of the thigh with respect to the hip is required to reduce errors and to increase the relevance of the method (Leardini et al; 1999, Delp et al; 1998).

Soft tissues and muscles move relative to the underlying femur bone in functional HJC determination. This adds soft tissue artefacts (STA) to the collected data. The effect of STA to the functional methods of locating HJC was demonstrated by Camomilla et al. (2006) through a simulation study using the mechanical analogue shown if figure.2.11

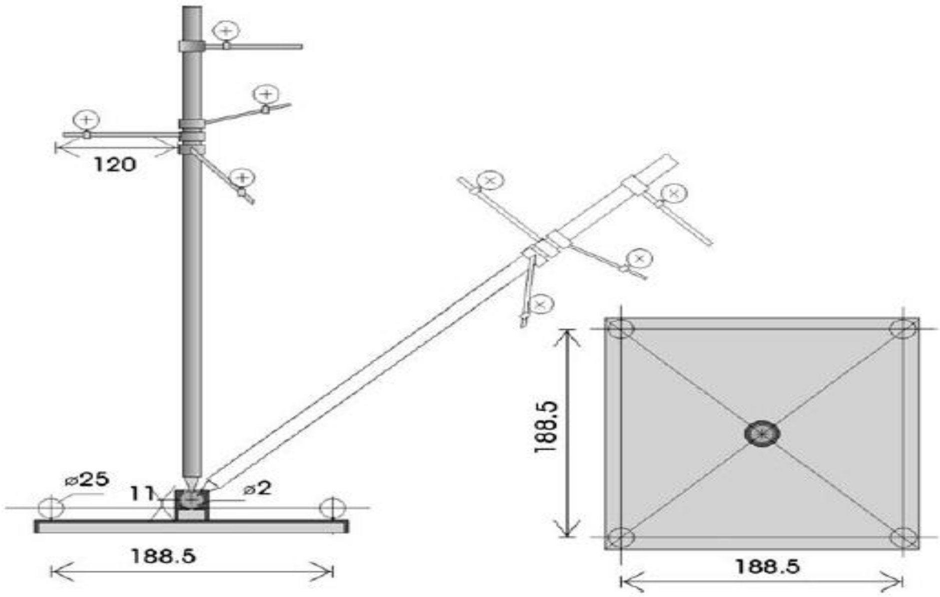

Figure 2.11: *Physical analogue of the femur-pelvis system. The construction allows for modification of cluster geometry. Measurements are in mm (From Cammomilla et al., (2006)*

The authors used the mechanical analogue to locate the HJC to 1mm error. In humans however, the functional technique often locates the HJC with error limits of up to 13mm (Leardini et al., 1999). Cammomilla and associates summarised the guidelines towards achieving best results as follows:

a. Use of quartic best sphere algorithm (developed by Gamage and Lasenby, 2002).
b. Star arc movement performed at self-selected pace. This is a sequence of abduction-adduction and flexion-extension femur movements followed by circumduction. All other possible movement patterns are shown in table 2.5 below. The cross movement was shown to give the worst result while the star is second to the star-arc.

Movement		Description
Cross	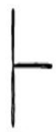	Flexion of 30°, neutral position, extension of 30°, neutral position, abduction of 30°, neutral position.
Circumduction		Flexion of 30°, half circumduction to extension of 30°, neutral position.
Star		Seven flexion-extension/abduction-adduction combined movements from the neutral position within the perimeter drawn in the *Arc* movement.
Star followed by arc		*Star* movement followed by *Arc* movement

Table 2.3: Description of lower limb (From Cammomilla et al., (2006)

c. Range or amplitude of movement should be as wide as possible.

d. Up to 500 data points should be sampled.

e. Centroid of markers should be located as close to the hip as possible.

f. Markers should be located at the greatest possible distance from each other.

The general assumption for all functional methods of locating the HJC is that the femoral markers or their centroid is fixed relative to centre of rotation. A class of analytical methods widely used in calculating the 3D location of the HJC does not impose geometrical constraints on the markers. In the analysis, each marker is assumed to lie on the surface of a sphere whose centre of rotation is coincident with the HJC. These approaches were implemented in the form of quadratic best sphere fitting (Cappozzo, 1984; Silaghi et al, 1991), quartic best sphere fitting (Gamage and Lasenby, 2002) and the Reuleaux method. The second class of analytical methods requires that the distance between markers do not vary ie, that the markers form a rigid cluster. The HJC is then estimated using least squares method, as the point on this rigid cluster that undergoes the minimum displacement with respect to the pelvic anatomical frame of reference frame.

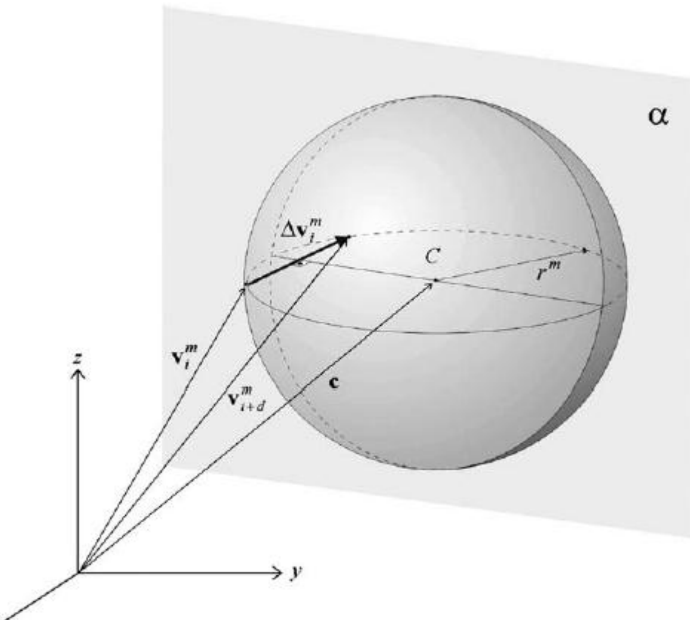

Figure 2.12: Shows the set x, y, z axes which are rigid relative to the proximal body segment (Pelvic anatomical reference). $v^m{}_i$ is position vector of the mth marker of the distal body segment at the ith sampled time. (Taken from Cereatti et al., 2006)

Algorithms for calculating the HJC from spatio-temporal data therefore:

a. Fits a geometrical sphere onto marker trajectories as in Leardini et al., 1999, SCoRE by Ehrig et al, 2011) and / or
b. Performs coordinate transformation to find the point that records the least motion with respect to global reference frame as in *Siston and Delp; 2006).*

2.8 VALIDATION TECHNIQUES

Validation techniques of locating the centre of the hip joint rely on medical imaging modalities such as the X-Ray, MRI, CT and ultrasound scanning. These techniques are known to give more accurate kinematic information and also have the advantage of being subject specific (Lenaerts et al; 2009). The major challenges in using them however, include high risk of ionizing radiation, cost and usual long processing times (Kainz et al; 2015).

2.9 PREVIOUS STUDIES INVOLVING THE USE OF ULTRASOUND IN DETERMINING THE HJC

Hicks and Richards (2005) implemented the ultrasonic technique of locating the HJC. Their study also reviewed the clinical applicability of functional techniques using sphere fitting algorithms. The main highlight of the study was the discovery of the potentials of the ultrasonic technique as a valid gold standard for comparing other methods of HJC determination. The simplicity of their experimental set-up and computations were also remarkable and imply that HJC can also be more conveniently determined by the ultrasound techniques than with the other methods. Measurements of the anterior femoral head were taken with the transducer probe in transverse and longitudinal orientations. In the transverse position, the anterior-posterior and medio-lateral views of the HJC were obtained while the longitudinal orientation enabled the sagittal plane view.

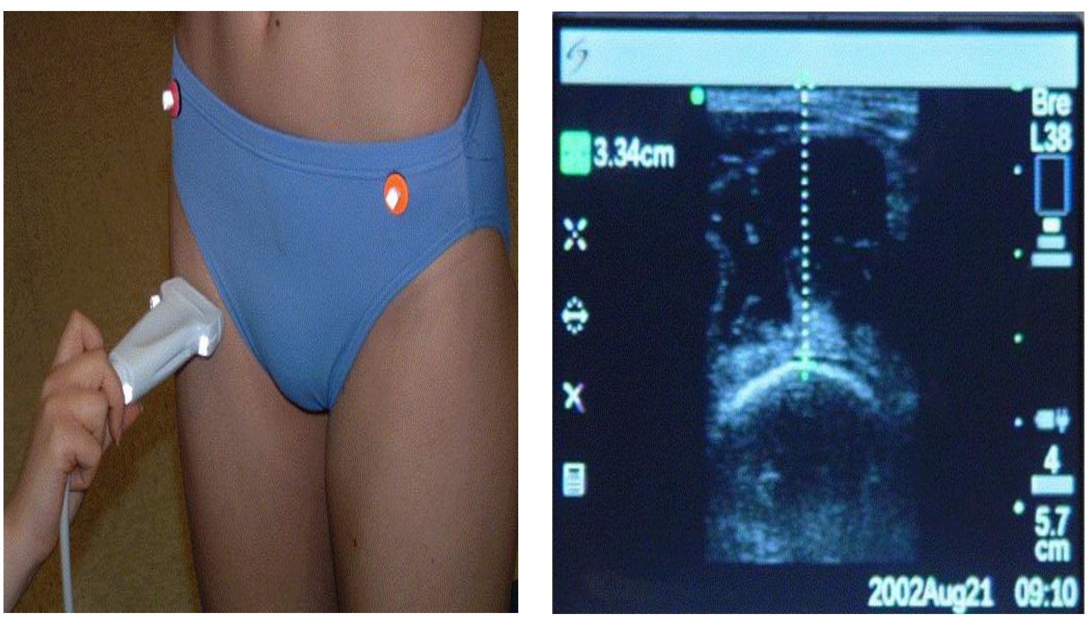

Figure 2.13: Ultrasound imaging of the hip to reveal the femoral head. Taken from Hicks and Richard (2004)

The images in figure 2.13 above display the pattern for marker placement and transducer probe orientation during measurement.

The HJC was calculated by fitting a circle to the arc formed by the femoral head using four points manually identified on the image. The distance between the probe and the centre of the circle was then calculated and multiplied by a unit vector representing the orientation of the probe during imaging. This made it possible to obtain the hip joint centre in the pelvic coordinate system. While being aware that error could be introduced to their result due to the uncertainty in identifying the widest arc projected by the femoral head, the authors still used the ultrasound technique as a gold standard. Fig 2.14 below shows how projections of the femoral head in an ultrasound image may lead to error if the arc projected by the scan line is not the greatest arc whose centre coincides with the centre of the femoral head.

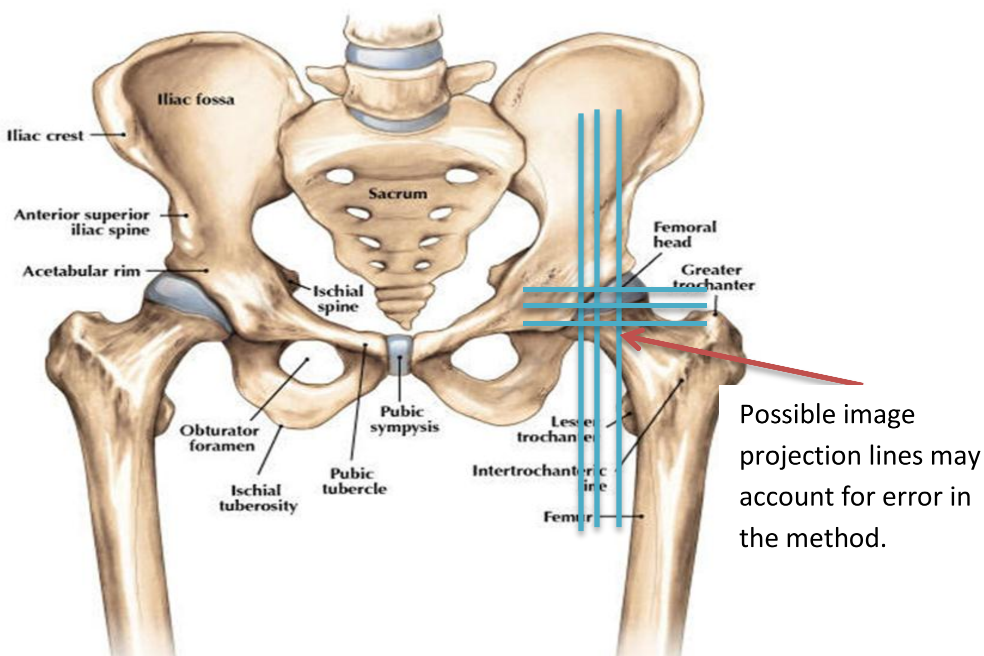

Figure 2.14: Image of the hip joint showing projections of the femoral head that can be captured in an ultrasound scan. (http://nick-carrington.co.uk/uploads/images/hip-anatomy.jpg)

determination of the probe's scan plane in relation to other reference markers. This was done by attaching retro- reflective markers to the probe. A Cambridge stylus was also used in a water bath during the calibration. The stylus was imaged from various known positions while inserted in the water bath. The images thus contained a set of points representing the stylus target. A transformation matrix was obtained by minimizing the least squares distance between identified points on the ultrasound image and the 3D locations of the stylus target in the water bath according to the following cost function:

$$f(t) = min \sum_{i=}^{m} \|T * USi - V\ i\|^2 \quad \text{……………………………….(2.14)}$$

Where USi = points identified on the ultrasound image

$V\ i$ = 3D locations of the stylus target in space at the same time image is taken.

Probe calibration enabled the determination of the coordinates of a 35mm diameter retro-reflective marker phantom placed in the water bath relative to those of three markers placed outside the bath. These markers were used as water bath reference frame. The authors ensured that the actual location of the phantom was noted before filling the tank with water. Images of the phantom were then taken with landmarks identified on them manually digitized. Least squares technique was again, used to determine the centre of the sphere. The coordinates of this centre was then translated into the water bath coordinate system and compared with its measured location. An accuracy of 4 ± 1mm was observed in the estimated phantom location. The study also scanned human subjects' hips. The participants stood erect with the scanned hip externally rotated. This was done to expose a greater fraction of the femoral head. The ultrasound probe was located with reference to the pelvic coordinate system using the two ASIS and PSIS markers. Least squares technique was then used to fit a sphere to the 30 landmarks manually digitized on the perimeter of the imaged femoral head. Their result for the HJC was validated using the MRI technique. However, since it was not possible to establish same pelvic coordinate system for the two modalities due to the different subject position during MRI scan, the authors used inter HJC as an index for their validation and got a mean difference of 4 ± 2mm difference.

2.10 VISIT OF THE UNIVERSITY OF DUNDEE

The University of Strathclyde has a culture of collaboration with the University of Dundee in some important biomedical engineering research interests. The visit was aligned to take advantage of that relationship to acquire more information from experts in medical physics, radiology and engineering which could facilitate the current study. The excellent interdepartmental research cooperation existing in the University of Dundee has been known to make trips of this nature highly informative and educative.

Consultation with Professor Corner was very valuable. He appreciated the major challenges of the current study which include:

a. How to position the subject to get access to the head of the femur given that it is deeply embedded in the acetabulum.
b. How to overcome ultrasound absorption and utilize the hyper-echoic nature of bone to get a trace of the femoral head which is embedded deeply in the acetabulum
c. How to specify the location of the hip joint centre in space relative to a suitable reference frame.

The Professor however advised that the knowledge base required to make the current study successful could be obtained through consultation of related literature and constant practice of ultrasound scanning using phantoms that mimic tissues. He offered to help with 3D printing of the femur and gave valuable information on preparation of polyvinyl acetate (PVA) tissue phantoms. Mr. Xiaowei Zhou, his Phd student working with both PVA and Agar phantoms demonstrated the procedure for preparing each type of phantom and emphasized the need to carry out the procedure in a fume cupboard to avoid inhaling particles. According to him, PVA phantom is made by mixing 18% by mass of PVA powder with 82% by mass of distilled water and then freezing and thawing the mixture for a number of times. The freezing and thawing cycles determine the mechanical properties of the resultant phantom. Mr. Xiaowei used the PVA phantoms and agar phantoms to simulate vein and bone respectively.

Interaction with Dr. Paul Prentice whose expertise is on the impact of cavitation in tissues was also vital. According to him, using ultrasound on subjects for extended durations could cause acoustic cavitation which may have cumulative dangerous effect on the human body. The United States National Council on Radiation Protection and Measurements (NCRP) holds similar view on ultrasound and in a published document noted that acoustic cavitation results when sound passes through an area that contains cavities or bubbles such as the intestine and lungs in the adult. The document also pointed out that other parts of the body can contain cavities and bubbles which could cause acoustic cavitation.

During cavitation, sound waves cause these bubbles to expand and contract in rhythm thereby transmitting a secondary non directional wave. Dr Prentice acknowledged that this secondary wave improve image quality especially by helping to spread injected contrast agents. However, the NCRP's document attributed the collapsing of bubbles to instantaneous local rise in temperature and pressure which has the potential to produce highly reactive free radicals and other toxic compounds that could theoretically cause genetic damage. Rapid contraction of bubbles that occurs during cavitation was also shown to possess the potency to create liquid micro jets that can cause cellular damage.

A consultant radiologist at the Nine-well hospital viewed the aim of this study as an impossible task. According to him, the ultrasound beam cannot penetrate the acetabulum to reveal the anatomy of the interface between it and the femoral head.

However, the current study intends to obtain the curvature of the femoral head through a small imaging window available from the anterior hip and to find the centre of a circle reconstructed from it. The centre of the circle will be coincident with the centre of the hip joint. Coordinate transformations will then be used to relate the centre coordinates to an appropriate reference frame.

2.11 CHAPTER SUMMARY

The anatomy hip joint was explored in this chapter. Basics of ultrasound and bone ultrasonography were also covered. The femoral head was shown to be embedded in the acetabulum and covered by cartilages, tendons and muscles .Ultrasound was found to be an imaging modality generated by pulsating crystals through reverse piezoelectric effect. Diagnostic ultrasound was seen to be limited in frequency. The type of probe used in scanning, the ultrasound frequency and impedance matching using ultrasound gel were emphasized as factors that contribute to the acquisition of quality images using ultrasound. The need for appropriate measures to eliminate cavitation during ultrasound imaging was also highlighted. Predictive and functional techniques of determining the hip joint centre were covered in the chapter. Previous studies on the use of ultrasound in locating the hip joint centre were also presented. The aim was to gain sufficient insight to select best parameters and methods to conduct the current study.

CHAPTER 3:MATERIALS AND METHODS

3.1 BACKGROUND

The need to develop a system that can be used in locating the hip joint centre (HJC) accurately as noted in previous sections triggered the development of the two popular classes of techniques in current use. Existing techniques already cited that applied ultrasonic technology did not present their methods with adequate clarity. Hicks & Richards (2005) particularly, acquired the ultrasound image in a manner that questions the possibility of obtaining an arc whose radius could competently be used to reconstruct the femoral head. The methods of the current study will aim to make the application of ultrasound to finding the HJC as convenient and accurate as possible. The feasibility of a method using the database of proximal femur anthropometric data together with ultrasound will also be tested. Finally, the results will be compared with those of predictive and functional techniques. MRI modality will be used to validate results.

3.2 EQUIPMENT

The attempt by Mona (2013) to locate the hip joint centre using ultrasound method was foiled by the inability to acquire clear images of the femoral head using the ultrasound equipment available to the department at the time. The study was therefore inconclusive. The present study however, makes use Analogic ultrasonix Q+ equipment and a twelve camera VICON motion capture system.

The ultrasound equipment (fig 3.1) has advanced research capabilities and features such as panoramic scan, elastography, colour Doppler imaging, sonic shine, measurement, ECG, 3D/4D imaging as well as B and M scan modes. The research capabilities enable the acquisition and storage of image in a variety of formats such as PNG, JPEG, DICOM, AVI e.t.c. It also comes with some third party software such as MATLAB® and permits modification of many imaging parameters and the use of operational modes that are not available in conventional clinical ultrasound equipment. These features however, come with extra license cost. The current study was carried out using a 38mm multi-frequency (5MHz to 14MHz) probe. Optimization of image was achieved by adjusting the time gain compensation, frequency, dynamic range, chroma, frame rate and depth. Figure 3.2 is a sample image of the hip obtained by ultrasound scanning.

Figure 3.1: Analogic Ultrasonix Q+ Equipment

Figure 3.2: Ultrasound image of the hip showing: 1. Iliopsoas muscle, 2. Acetabular rim and 3. Femoral head, Nestorova, et al., (2012).

The VICON system used is consisted of 12 cameras. The system's infra-red marker tracking system enables high resolution reconstruction of kinematic and kinetic data associated with human motion. Kinetic data such as joint reaction forces and moments could be obtained if a force plate was connected to the system.

The VICON Nexus software which accompanies the motion capture system provides the platform for data acquisition in various formats such as the comma separated variables (csv), c3D, avi etc. The software has an efficient database management tool known as Eclipse which neatly organises subjects, sessions and trials as nodes. It was also possible to play back in 3D, captured and reconstructed marker trajectories of subjects.

3.3 EXPERIMENTAL DESIGN

The experiment was carried out in phases. The first phase was familiarization with the ultrasound equipment. Various imaging techniques were utilized to explore ways through which the improved functionality of the equipment can aid in the development of convenient, easy and accurate methods of locating the hip joint centre in 3D space. During this phase, several images were captured using combinations imaging features. Frequency, dynamic range, frame rate, map time gain compensation and chroma were adjusted while the use of measurement facility and centre line were found to be a suitable means of discretizing points on the periphery of the femoral head. Fig 3.3 shows images of the femur head and a panoramic image of anterior fore-arm showing the ulna bone captured during this phase. The image also displays the combination of settings used during its acquisition. Aquasonic 100® ultrasound transmission gel was used. It is hypoallergenic and water soluble and has commendable skin impedance matching capability. Another type of gel used gave very poor results. This highlights the importance of using proper ultrasound gel during imaging.

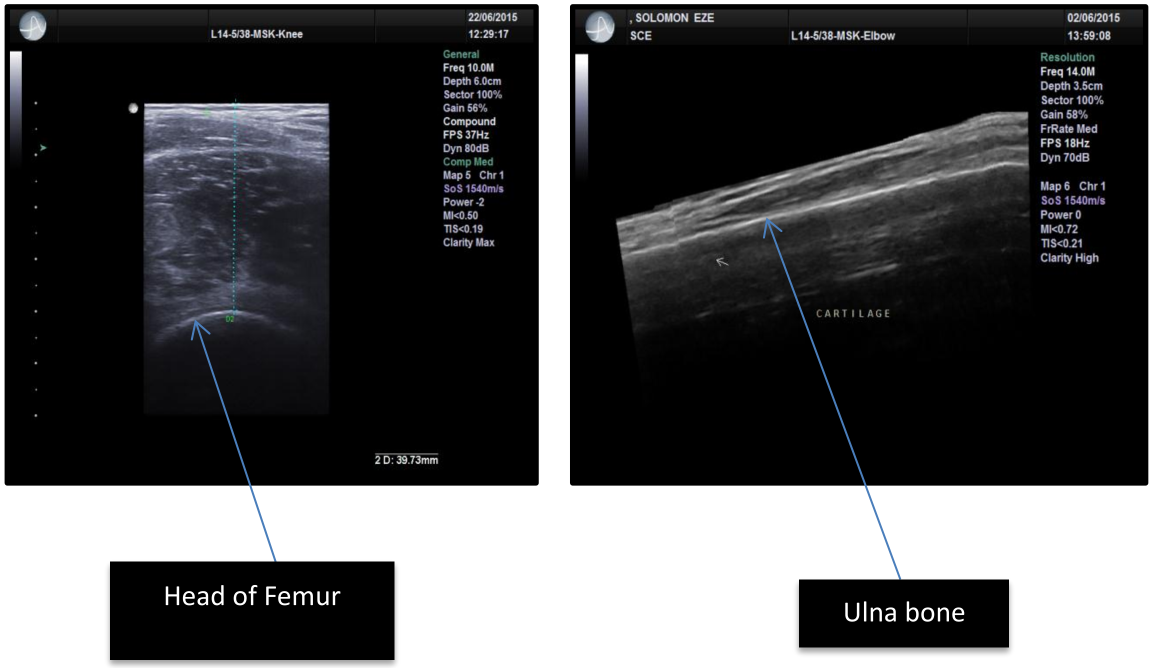

Figure. 3.3: Ultrasound images of the femur head and ulna bone. Image also show combination of settings used to acquire the image

The second preparatory phase of the study was the design and production of tissue phantom in a plastic container. This was conducted to determine if the speed of sound ‘C’ varied significantly within the tissue medium since the distance measured from the tip of the ultrasound probe to the femoral head would depend on the velocity of ultrasound propagation. The acoustic property of the phantom material was found to match that of the human tissue.

The material used in tissue phantoms because of its excellent tissue mimicking properties is polyvinyl alcohol (PVA) hydrogel. Generally, to prepare a tissue phantom based on PVA, about 10 wt % of the adhesive powder is dissolved in water (T Hatakeyama et al, 2005). The mixture is then subjected to several cycles of freezing and thawing. This process determines the texture of the final phantom. For this study, a commercial paper adhesive ‘Solvite ® all-purpose paper adhesive’ was used. This was much less expensive than PVA made for laboratory use. Approximately 170g of the adhesive was mixed in 1700g of water. The mixing was carried out in a fume cupboard and continued until a homogenous pasty mixture was obtained. The mixture was then cast into a container in which a Sawbone ® femur phantom was fixed. The 3D position of the femoral head of the phantom with respect to one end of the container is as shown in figure 3.4. Casting was done with caution to avoid altering the phantom femur position. The resultant phantom was then subjected to three cycles of freezing (-80^{o}C) and thawing. The freezing took three hours while thawing took 24 hours. The Solvite ®adhesive contains fungicide which helps to protect it against mold growth. The handling was therefore done carefully and hands washed thoroughly with soap after each occasion.

A training course on data capturing using the VICON motion capture system was the final preparatory phase. This was essential since the study required getting 3D position data. In order to prepare the system for data capturing, the following sequence was followed:

a Systems preparation.
b. Subject preparation
c. Capture
d. Gap filling
e. Output
f. Analysis

System preparation entails powering the VICON motion camera, booting the computer, loading the Nexus software, aiming the cameras and calibration. For a VICON system that has been in use as encountered in this study, only calibration was non-trivial. Calibration was done to allow the software to determine the position and orientation of all the cameras. It was also done to diminish errors in the calculation of marker trajectories.

Two types of calibration were done: dynamic and static. The aim of dynamic calibration was to enable the system determine the relative position and orientation of each camera as well as to linearize them for accuracy. Dynamic calibration was done by waving a calibration wand bearing same type and size of markers as would be used in the actual test. The VICON Nexus was maintained in 'live' mode during calibration.

The static calibration on the other hand, determines the centre or the origin of the laboratory volume and its orientation. A screen shot photograph of a calibrated gait laboratory is shown in figure 3.5 along with that of a calibration wand.

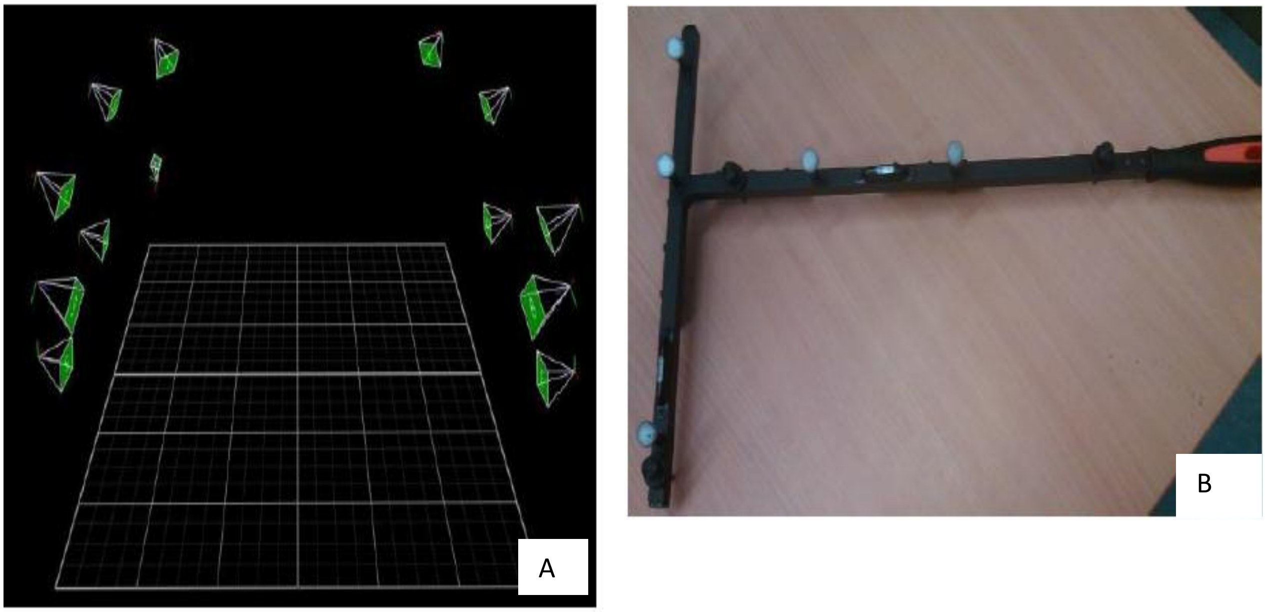

Fig 3.5: A. Screen shot of a calibrated laboratory and camera positions. B. Calibration wand

3.4 ULTRASOUND DATA COLLECTION

Five subjects whose body mass indices (BMI) were less than 26.5 volunteered to participate in the study in accordance with the ethical approval (Appendix D). After calibrating the laboratory, anthropometric data of each participant (age, sex, height, leg length, knee width, as well as inter ASIS and PSIS distances) were recorded. An Eclipse ® folder was then created for the session and nodes were used to depict each subject's name. Having created the session and activated it, 14 mm retro-reflective markers were attached to the ultrasound probe and to both ASISs and PSISs of the first subject. Following this, each subject was asked to walk into the capture volume and stand near the ultrasound equipment while Nexus was set to 'live' mode. A few frames were captured by pressing the capture button. Nexus automatically went offline when the stop button was pressed after one second, to stop the data capture. The data were used to reconstruct the trial in 3D. Two segments were formed: one with the markers on the two ASIS and

PSIS and the second with the three markers on the probe. The segments were then labeled, linked with a free joint and saved. The subject was made to stand with the leg to be scanned (right leg) fully rotated outwardly. Ultrasound images of the hip were recorded for four seconds at 200Hz while the VICON system tracked the positions of the probe and subject's hip. An assistant operated the VICON Nexus and was signaled to start and to stop when required. This was repeated three times each for all the subjects one two and three in quick succession. Only one trial each was successfully recorded for subjects four and five. In each trial, the measurement facility of the ultrasound equipment was used to discretize a minimum of five points on the arc of the femur head and to measure the distance between the apex of the arc and the surface of the probe. A reconstructed image showing the subject's pelvis and the probe is presented in fig. 3.6. MATLAB® code was used to implement a least squares sphere fit to determine the centre of the femoral head relative to the probe and to perform coordinate transformation to relate it to the pelvic reference frame.

3.5 DATA COLLECTION FOR THE FUNCTIONAL TECHNIQUE

Collection of data for the functional technique required attaching four additional markers to the thigh in addition to the four pelvic markers used to identify the anthropological landmarks of the pelvis. The thigh markers were attached arbitrarily between the hip and two third the length of the thigh. This was in agreement with Camomilla et al., (2006) who noted that fixing the thigh markers as close to the hip as possible and as radially apart as possible reduced error in the estimation of the HJC. Database and segments were also created as in the ultrasound technique explained above. However, the segments were linked with a ball and socket joint which closely models the hip joint. It should be noted that the type of joint used to link the two segments does not really have effect on the trajectory data which are simply 3D positions attained by the markers as the leg is moved in the pre-determined pattern. Trial data were captured while the subject moved his leg in star-arc pattern. The star-arc movement refers to a sequence of abduction-adduction, flexion-extension and circumduction. The trial data were captured at 100 Hz, reconstructed and outputted in .c.s.v and c3D formats for further processing to determine the HJC in pelvic reference frame. These steps were repeated for the other two subjects.

3.6 ALGORITHM DEVELOPMENT FOR THE ULTRASOUND METHOD

Ultrasound images of each subject's head of femur were digitized using the measurement facility of the equipment. The discretized points (as shown in figure 3.6) are then manually inputted into a MATLAB ® circle fitting programme to determine the location of the centre of circle corresponding to the centre of the femoral head in the transducer frame of reference.

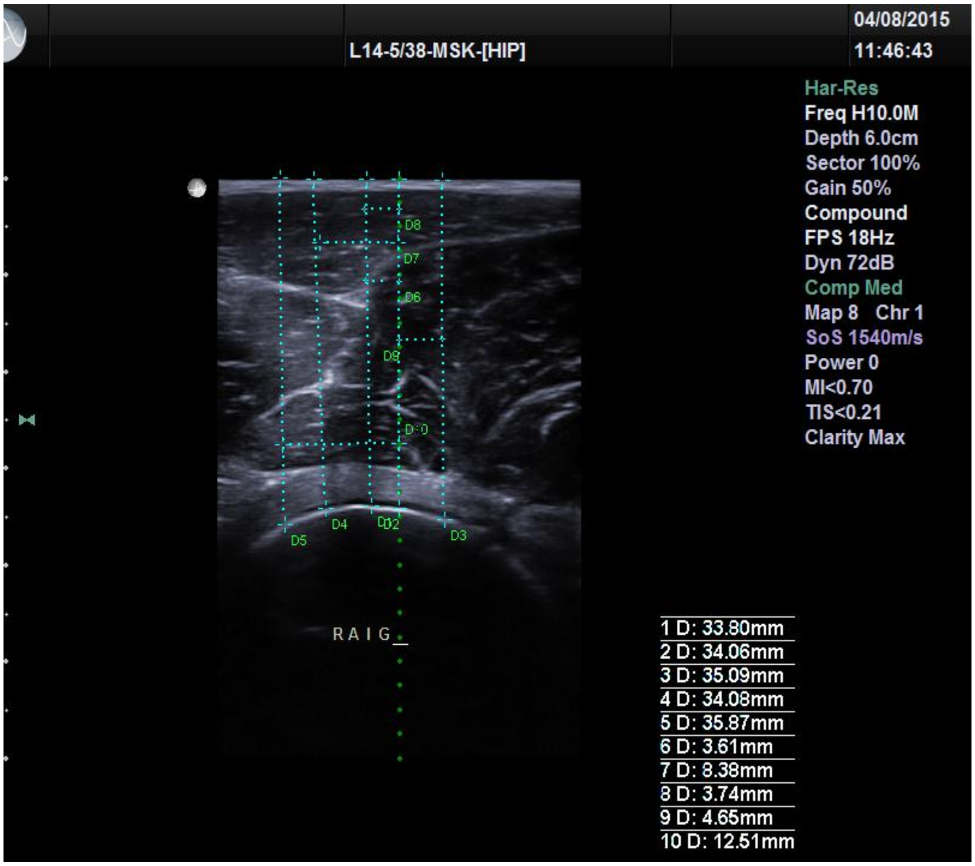

Figure 3.6: Ultrasound image showing how the surface of the femoral head was discretized.

The centre of the circle in the ultrasound probe's reference frame is then transformed into the global reference by means of the coordinate values of three markers attached to the ultrasound probe as shown in figure 3.7. The coordinates of the three markers were sufficient to define the probe's orientation in the global frame of reference. This also made it possible to relate the centre of the fitted circle in terms of global reference frame.

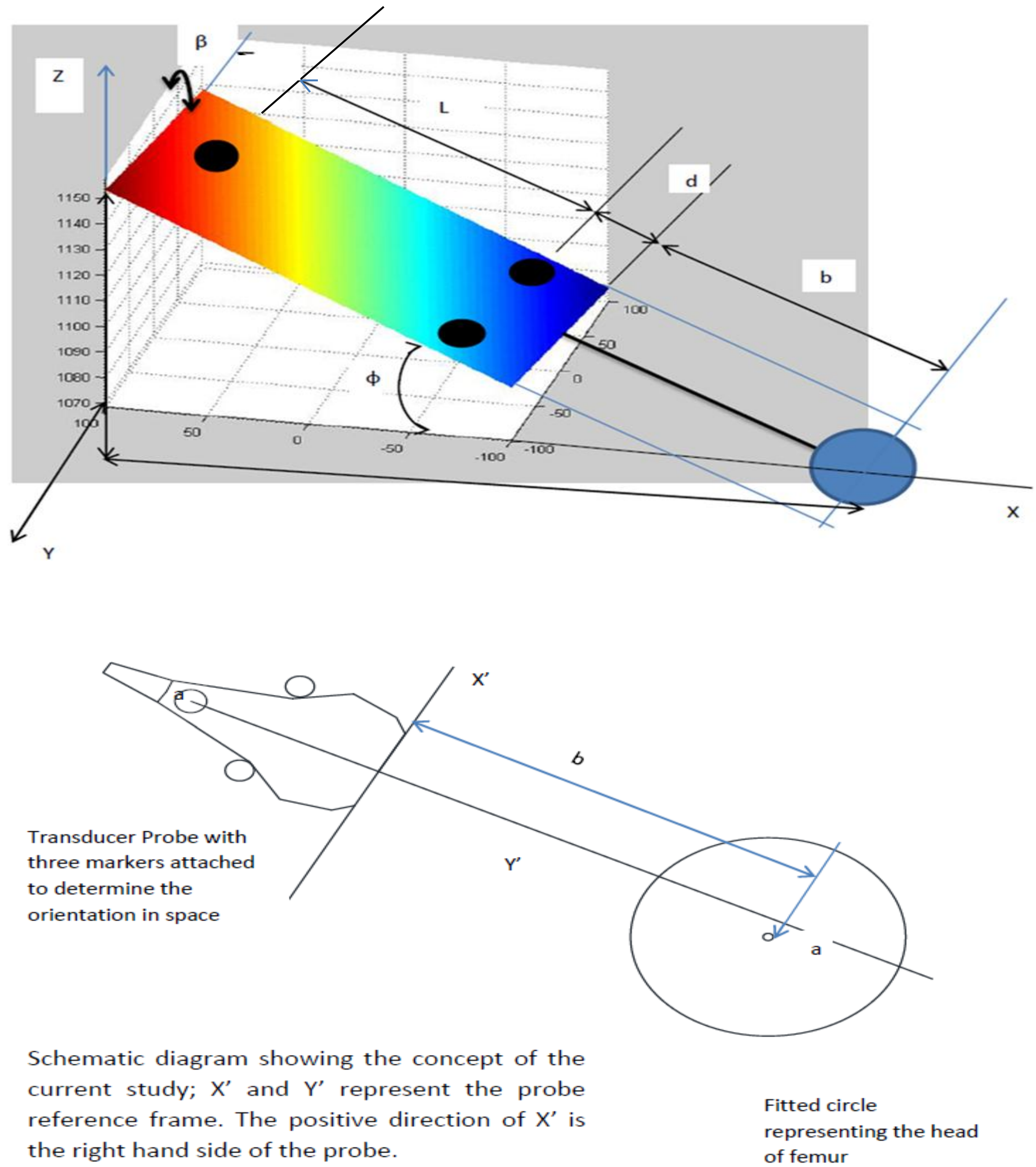

Figure3.7: Schematic diagrams showing the orientation of a plane in space. The planar images represent the ultrasound transducer probe and the femoral head.

The exact positions of the probe markers are shown in figure 3.8.

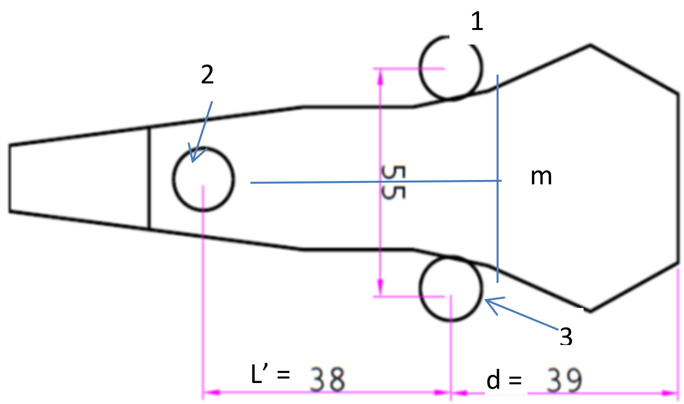

Figure 3.8: Marker positions on the ultrasound transducer probe. The point m, is the midpoint between markers 1 and 3.

In the analysis, the coordinate of the midpoint between markers 1 and 3 is collinear with those of markers 2. This reduces the analysis to a simple linear one. In the X – Z plane therefore, the ultrasound probe and HJC may be schematically represented as shown in figure 3.9 below.

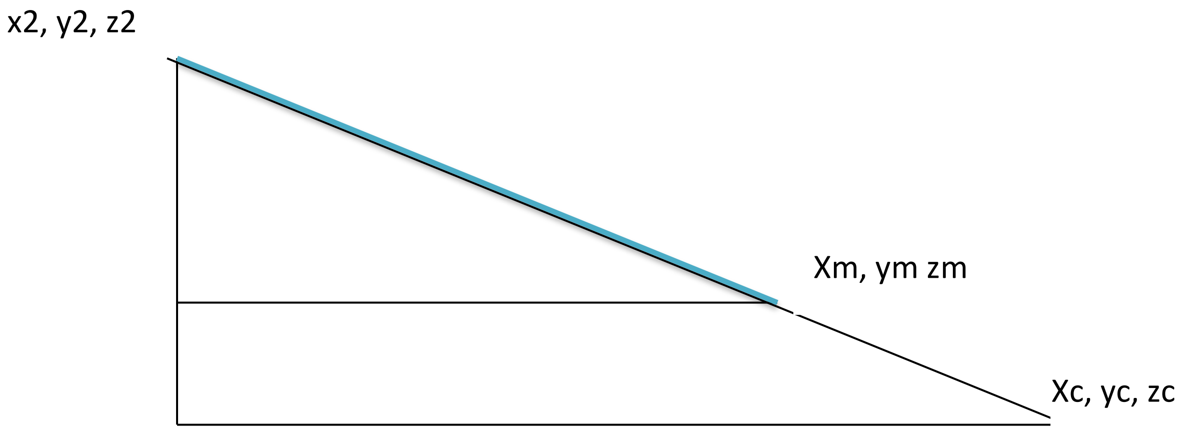

Figure 3.9: Linear view of the probe. Xc, yc, zc are the coordinates of the HJC in global coordinate system while xm, ym, zm are the coordinates of the midpoint between markers 1 and 3.

A relationship between the coordinates on the points indicated can be obtained using similar triangle. It can therefore be observed that:

$$\frac{z2 - zm}{L + d} = \frac{z2 - zc}{(L + d + b)}$$

This implies that:

$$zc = z2 - \frac{(z2 - zm)(L + b + d)}{L + d}$$

In the above equation, zm is the z component of the midpoint of the line joining markers ‘1’ and ‘3’ while zc is the Z-component of the HJC in the global reference frame. Marker

‘2’ was attached on the face of the probe. The actual z2 was therefore corrected to account for the height difference. Figure3.10 below shows the concept.

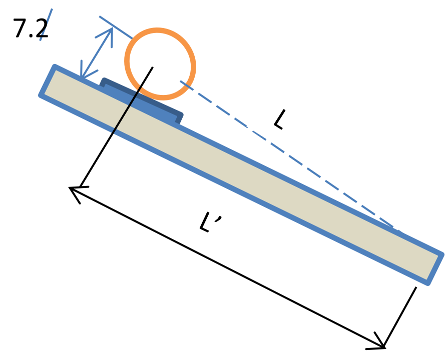

Figure 3.10: Shows height difference between markers. The actual length L, is computed using Pythagoras’ theorem

L = the actual length, representing interval between the markers. This is to be used in computations. L’ is the measured distance. L is computed by Pythagoras’s theorem as:

$$L = \sqrt{L'^2 + 7.2^2}$$

With L’ = 38, we have: L = 38.68mm

The correction thus accounts for the offset of marker ‘2’ with respect to markers ‘1’ and ‘3’.

By making appropriate substitutions (see figure 3.9), the Y- and X- components of the HJC is calculated with respect to the global reference frame as follows:

$$xc = x2 - \frac{(x2-xm)(L+b+d)}{L+d}$$

and,

$$yc = y2 - \frac{(y2-ym)(L+b+d)}{(L+d)}$$

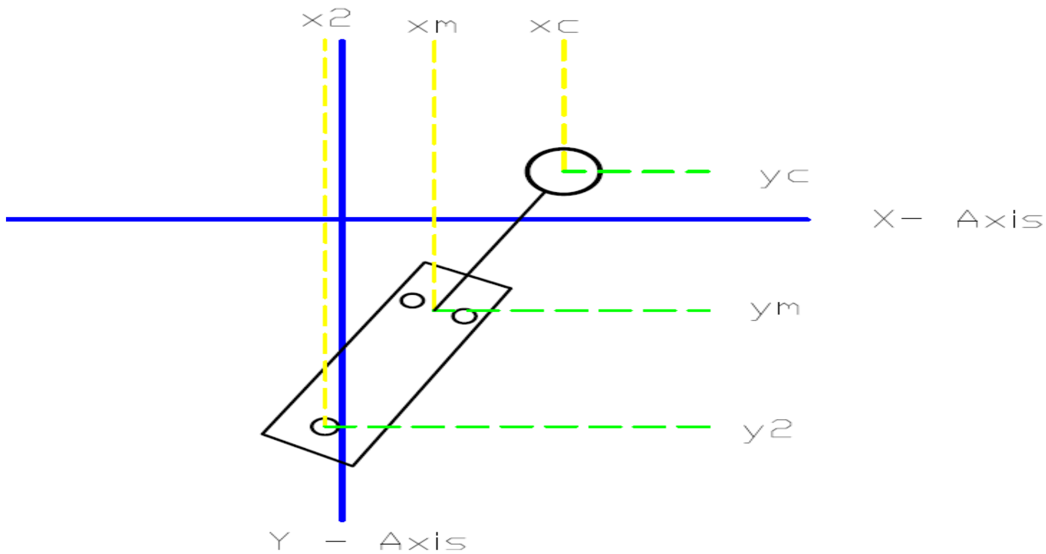

Figure 3.11: Schematic diagram showing the orientation of the probe in the X- Y plane

The coordinates of the HJC in global reference frame can therefore be determined by simply substituting the values of L and d. The other quantity b, is obtained after fitting a circle with the discretized points on the femoral head.

MATLAB® code developed in Simpson (2011) was modified and used to handle the data generated by the functional technique. The code was based on the 'quartic least square best sphere fit' algorithm developed by Gamage and Lasenby (2002). An important feature of this algorithm is that it handles all the data points once to generate the centre of rotation which is the HJC.

The HJC was determined with respect to the global coordinate reference. However, the algorithm developed for the functional technique gives the HJC in the pelvic anatomical reference. Since this study also aims to compare both results, coordinate transformation must be done to synchronize the reference frames prior to comparison.

The data collected from participants were carefully analysed to get results. Findings for the ultrasound technique will first be presented followed by those of the functional and predictive techniques. However, as the techniques gave the HJC in different coordinate reference frames, some coordinate transformations will be done to synchronise the results so as to enable comparisons.

3.7 COORDINATE TRANSFORMATIONS FOR THE ULTRASOUND TECHNIQUE

Throughout the tests, there was no interest in the position of the subjects as well as the ultrasound probes. The aim was to explore the possibility of using ultrasound to locate the HJC from any location within a calibrated volume such as that of a gait laboratory. Discretized femoral head images of the subjects were used to fit circles relative to ultrasound probe reference frame. Table 3.1 presents the results obtained.

Participant number	Femoral centre to probe midpoint distance, b (mm)	Radius of femur, R (mm)	R.m.s offset from centre line, a (mm)
1.	63.43 ± 2.20	22.05 ± 2.14	0.56
2.	59.20 ± 3.92	22.35 ± 2.00	3.29
3.	64.60 ± 4.28	25.51 ± 4.18	3.55
4	56.00	22.91	0.92
5	60.56	23.08	0.98

Table 3.1: Values (± S.D) obtained from discretising the ultrasound images of the femoral head.

A MATLAB code (Appendix A) was used to implement circle fitting using Pratt's geometrical circle fitting algorithm. The basic assumption in the computation was that the hip joint centre and the line through the midpoint of the ultrasound probe lie in a straight line. Thus subject trials whose offset values were greater than 1.5mm were not used. The values obtained for b were used in the MATLAB (Appendix B) code to calculate the coordinates of the HJC in terms of the Cartesian coordinate system of the laboratory ground. The HJC has to be expressed with respect to a dynamic reference frame for it to be applied in biomechanical calculations. To achieve this, coordinate transformation is used to relate the Cartesian global coordinate system of the calibrated volume into an anatomical coordinate system. This can either be done geometrically or by vectors. This analysis used the vector method.

A MATLAB code (appendix B) was also used to transform the HJC obtained in terms of the ground reference frame (GRF) of the gait laboratory to pelvic anatomical coordinate (PAC) system. The origin of the PAC system was located at the midpoint of the inter ASIS span with the Z-axis pointing in the inferior-superior direction, the X- axis, through the midpoint of the two PSISs; intersecting the inter ASIS span at midpoint (anterior-posterior direction). The Y-axis is in the medio-lateral direction. This is illustrated in figure 3.12.

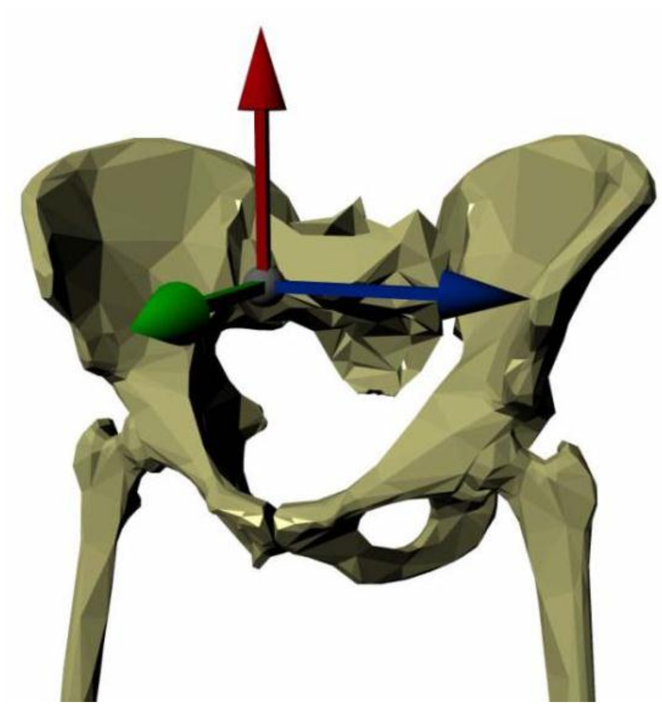

Figure 3.12: The Pelvic anatomical Coordinate system. The direction indicated in red is Z-axis while the green and blue are X- and Y-axes respectively. Image is taken from VICON Plug in gait manual

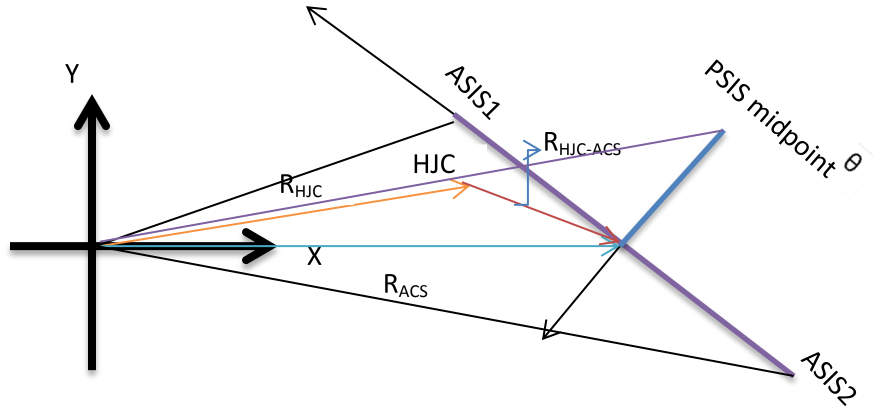

Figure 3.13: Schematic diagram showing the global and anatomical reference frames in 2D. The figure shows the vector relationships between the pelvic anatomical landmarks and the hip joint centre.

Vector operations were used to simplify the coordinate transformation by expressing the coordinates as unit vectors. The component of the HJC in each of the anatomical axes was then calculated by evaluating the projection or dot product of the vector through the HJC to origin of the anatomical reference frame (this coincides with the midpoint of the inter ASIS span) and the unit vectors defining each of the axes. The vectors defining the location of the HJC in the GRF are shown in figure 3.13. From the figure,

$$R_{HJC\text{-}ACS} = R_{ACS} - RHJC \quad \text{..} (3.1)$$

Evaluation of the dot product between the unit vectors defining the anatomical axes and the vector $R_{HJC\text{-}ACS}$ gives the coordinates of the HJC in the PAC system. The x, y and z components are as depicted in figure 4.2. The calculation below shows the methodology used to transform the global HJC coordinates of subject1 to pelvic anatomical coordinate system

Step1: subtract LASIS from RASIS to get medio-lateral axis (y)

$$\rightarrow r1 = (-1146.17i - 407.861j + 1073k) - (-926.205i - 301.576j + 1090.3k)$$

r1 = -219.965i -106.284j – 16.6k

The associated unit vector = $\frac{-219.965i - 1065.248 - 16.6k}{\sqrt{-219.965^2 + 106.284^2 + 16.6^2}}$

v1 = -0.8983i -0.434j – 0.0678k

Step2: Subtract PSIS from inter ASIS midpoint coordinates to get the Anterior posterior axis (x).

PSIS = ((-1160i – 210.342j + 1138.16) + (-1076.67 – 166.036 + 1143.38))/2

PSIS = -1118.335i – 188.18j + 1140.77k

ASIS midpoint = ((-1146.17i – 407.861j + 1073.7k) + (-926.205i -301.576j+1090.3k))/2

ASIS midpoint = -1036.185i – 354.72j + 1082k

PSIS –ASIS midpoint = r2 = (-1118.335i – 188.18j + 1140.77k) – (-1036.185i – 354.72j + 1082k)

r2 = -82.15i + 166.54j + 58.77k

Step3: Take the cross product between r1 and r2 to define an orthogonal axis (z):

$$\rightarrow \begin{matrix} i & j & k \\ -0.8983 & -0.434 & -0.0678 \\ -82.15 & 166.54 & 58.77 \end{matrix}$$

$$= -14.2148i + 58.3629j - 185.256k$$

Its associated unit vector is: *v2* = -0.0727i + 0.299j – 0.951k

The third coordinate axis is orthogonal to the first two; ie:

$$v3 = v2 \times v1 = \begin{matrix} i & j & k \\ -0.0727 & 0.299 & -0.951 \\ -0.8983 & -0.434 & -0.0678 \end{matrix}$$

$v3 = -0.4332i + 0.8496j + 0.3009k.$

The coordinates of the PAC system are therefore defined as follows:

$$\begin{bmatrix} ePx \\ ePy \\ ePz \end{bmatrix} = \begin{matrix} -0.4332 & +0.8496 & +0.3009 \\ -0.8983 & -0.434 & -0.0678 \\ -0.0727 & 0.2991 & -0.951 \end{matrix} \begin{bmatrix} i \\ j \\ k \end{bmatrix}$$

The HJC was obtained in the ground reference frame (GRF) as:

-931.4i -312.8j + 1037.5k

The displacement of the HJC from the origin of the new coordinate system is:

(-931.4i -312.8j + 1037.5k) – (-1036.185i – 354.72j + 1082k)

= 104.785i +41.12j -44k

ePx = (104.785i +41.12j -44k).(-0.4332i +0.8496j + 0.3009k)

= -*23.697*

ePy = ((*104.785i +41.12j -44k).(-0.8983i - 0.434j - 0.0678k)*

= -*109.311*

ePz = (104.785i +41.12j -44k).(-0.077i + 0.2991j - 0.951k) = - *47.2128*

$$\rightarrow HJC = \begin{bmatrix} -23.697 \\ -109.311 \\ -47.2128 \end{bmatrix} \text{mm for the subject}$$

Where ePx, ePy and ePz are components of the HJC in the three pelvic anatomical axes. A MATLAB code (Appendix C) was used to implement the calculation for the other subjects.

CHAPTER 4: RESULTS

4.1 RESULTS FROM THE ULTRASOUND TECHNIQUE

The methodology and sample calculation used to derive results for the ultrasound method has been shown in chapter three. This chapter aims to present the results from the three techniques namely: ultrasound method, functional method and predictive method. These are as summarized in table 4.1. As shown in the table, the displacement of the HJC medial to the ASIS in all the trials maintains a remarkable consistency. The fifth trial was somewhat awkward, indicating that the HJC was located lateral relative to the ASIS. Possible causes of this error could be wrong location of the ASIS and relative movement of overlying tissue during imaging.

4.2 RESULTS FROM THE FUNCTIONAL TECHNIQUE

The essence of conducting the functional technique was to compare results obtained from the two techniques since literature has reported various accuracy limits for the two. The MATLAB code used to process collected data expresses the hip joint centre in pelvic coordinate system. This simplified the task.

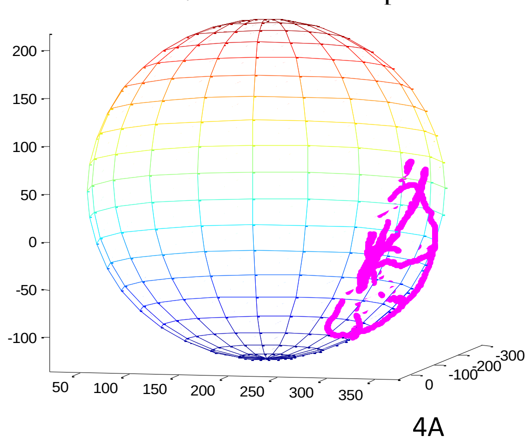

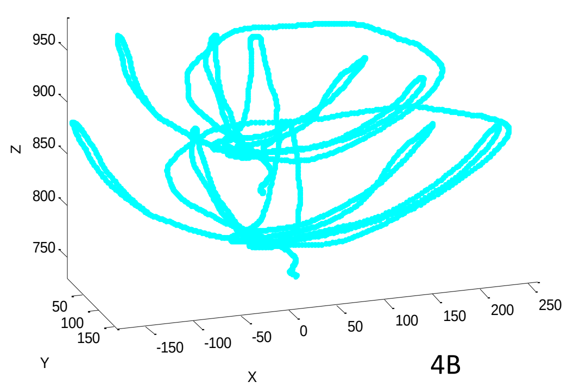

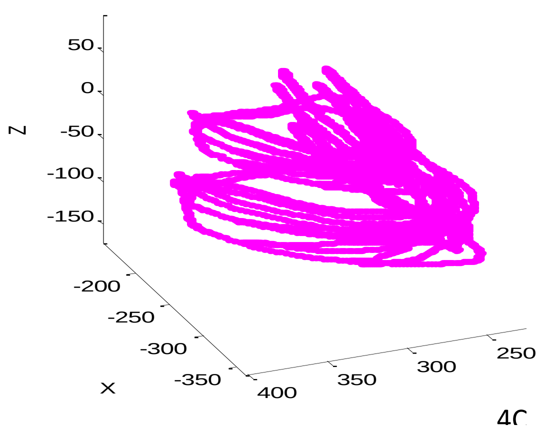

Figure 4.4: Trajectories of markers attached to the thigh during the Functional test. 4A shows a single marker's trajectory in relative coordinate system as in 4B, but enclosed in its sphere. 4C displays the collective markers' trajectories in millimetres.

In the functional tests, the thigh markers were attached towards the proximal part of the thigh. This was done to take advantage of the recommendations made by Camomilla et al., (2005). The tested limb was also moved in star –arc motion as contained in the paper. The trajectories of the thigh markers are shown in figure 4.4. The results obtained from the functional tests using this approach were fairly consistent, especially in the medio-lateral axis. The results are as follows:

First subject's trial gave HJC at:

$$\begin{bmatrix} -15.4273 \\ -113.302 \\ -9.723 \end{bmatrix} \text{mm}$$

For the second subject, trial yielded HJC at:

$$\begin{bmatrix} -40.6648 \\ -118.7723 \\ -0.2789 \end{bmatrix} mm$$

For the third subject, trial gave HJC at:

$$\begin{bmatrix} -36.0996 \\ -123.1986 \\ -27.4312 \end{bmatrix} \text{mm}$$

And the fourth subject's HJC was located at:

$$\begin{bmatrix} -36.061 \\ -114.0451 \\ -9.0451 \end{bmatrix} \text{mm}$$

While the fifth subject had his at

$$\begin{bmatrix} -7.262 \\ -134.681 \\ -24.674 \end{bmatrix} \text{mm}$$

4.3 RESULTS FROM THE PREDICTIVE TECHNIQUE

Harrington et al proposed a set of relational equations for locating the HJC. Their equations are highly recommended by the ISB. It was therefore necessary that results of the current study be compared with theirs. The equations are:

$X = -0.24PD - 9.9$

$Y = -0.30PW - 10.9$

$Z = 0.33PW + 7.3$

X, Y and Z are consistent with the PAC system defined. A negative value in the Y-direction only gives a sense of whether the right or left HJC is being referred to.

Substituting the values of PD and PW for subject 3,

$X = -0.24(188) – 9.9 = -55.02mm$

$Y = 0.33(245) + 7.3 = 88.15mm$

$Z = -0.30(245) – 10.9 = -84.4mm$

Results for all trials, using the Harrington’s method are summarized in table 4.1

The positive or negative sign accompanying the HJC coordinate values indicate whether the side tested is the right or left hip in them Y- or medio lateral component. Thus, only the absolute value is relevant. The results from the three tests are summarized in table 4.1 below.

Subject	Inter ASIS distance or PW (mm)	PSIS to PW distance midpoint or PD (mm)	Ultrasound Result (mm)	Result from Functional Technique (mm)	Predictive Technique (mm)
1.	244.9	194.8	$\begin{bmatrix}-23.70\\-109.31\\-48.53\end{bmatrix}$	$\begin{bmatrix}-15.43\\-113.30\\-9.72\end{bmatrix}$	$\begin{bmatrix}-56.65\\88.18\\-84.40\end{bmatrix}$
2.	193.3	174.0	$\begin{bmatrix}-20.25\\-85.62\\-83.44\end{bmatrix}$	$\begin{bmatrix}-40.67\\-118.77\\-0.28\end{bmatrix}$	$\begin{bmatrix}-51.66\\71.09\\-68.90\end{bmatrix}$
3.	245.0	188.0	$\begin{bmatrix}-40.469\\-109.50\\-64.472\end{bmatrix}$	$\begin{bmatrix}-36.100\\-123.20\\-27.43\end{bmatrix}$	$\begin{bmatrix}-55.02\\88.15\\-84.40\end{bmatrix}$
4.	242.1	218.8	$\begin{bmatrix}-14.93\\-101.13\\-58.65\end{bmatrix}$	$\begin{bmatrix}-36.06\\-114.36\\-9.045\end{bmatrix}$	$\begin{bmatrix}-62.20\\87.16\\-83.53\end{bmatrix}$
5.	246.5	195.0	$\begin{bmatrix}-21.71\\-126.54\\-54.02\end{bmatrix}$	$\begin{bmatrix}-7.26\\-134.68\\-24.67\end{bmatrix}$	$\begin{bmatrix}-56.70\\88.64\\-84.89\end{bmatrix}$

Table 4.1: Summary of results obtained from ultrasound, Harrington's predictive and functional hip joint centre determining tests.

CHAPTER 5: DISCUSSION

The results summarized in table 4.1 readily shows that the three techniques used in locating the HJC gave different results. It was necessary to validate the results. However, result validation demands a suitable gold standard such as MRI imaging for all the subjects. This was not possible in current study due to cost constraints.

In the literature, Leardini et al.,(1999) noted that results obtained from functional techniques can be in error by up to 13 mm while those of predictive techniques can be as much as 25 to 30mm in error. However, Sangeux et al., (2011) validated various algorithms used in functional methods and the regression equations of selected predictive techniques. Their results showed that sphere fitting algorithm located the HJC to a mean absolute error of 20mm in 85% of their measurements while the Harrington's regression equations gave the HJC to 20mm absolute error in 88% of the measurements. Peters et al., (2010) found a mean absolute inter HJC displacement of 4 ±2mm between HJC obtained using MRI and those with 3D ultrasound. These results indicate that functional techniques, especially those using the sphere fitting algorithm perform better than the Harrington's predictive technique while the ultrasound method compared closely to MRI.

The quartic sphere fitting algorithm proposed by Gamage and Lasenby was used in the current study and guidelines recommended by Camomilla et al., (2006) were also observed. The results shown in table 5.1 compares the HJC coordinates calculated from the ultrasound method with those of functional and predictive techniques. From the table, it can be observed that results from ultrasound and functional techniques were within 15mm interval in the medio-laterial and anterior-posterior directions for the first, third, fourth and fifth subjects. In the inferior-superior direction, the results obtained from the two techniques showed greater differences. The results obtained for subject 2 had the greatest difference. During the data collection stage for functional technique, some of the trajectory data were lost. These were filled using spline function of the Nexus software.

Subject	Ultrasound Technique results (mm)	Functional Technique results (mm)	Predictive Technique (mm)	Absolute difference between ultrasound method and Functional method $\begin{bmatrix}\Delta x\\ \Delta y\\ \Delta z\end{bmatrix}$ (mm)	Absolute difference between ultrasound method and Predictive method $\begin{bmatrix}\Delta x\\ \Delta y\\ \Delta z\end{bmatrix}$ (mm)
1	$\begin{bmatrix}-23.697\\ -109.311\\ -48.532\end{bmatrix}$	$\begin{bmatrix}-15.4273\\ -113.302\\ -9.723\end{bmatrix}$	$\begin{bmatrix}-56.65\\ 88.18\\ -84.4\end{bmatrix}$	$\begin{bmatrix}8.270\\ 3.709\\ 38.809\end{bmatrix}$	$\begin{bmatrix}32.953\\ 21.131\\ 35.648\end{bmatrix}$
2	$\begin{bmatrix}-20.247\\ -85.620\\ -83.443\end{bmatrix}$	$\begin{bmatrix}-40.665\\ -118.772\\ -0.279\end{bmatrix}$	$\begin{bmatrix}-51.66\\ 71.09\\ -68.9\end{bmatrix}$	$\begin{bmatrix}20.418\\ 33.152\\ 83.164\end{bmatrix}$	$\begin{bmatrix}31.413\\ 14.53\\ 14.543\end{bmatrix}$
3	$\begin{bmatrix}-40.469\\ -109.502\\ -64.472\end{bmatrix}$	$\begin{bmatrix}-36.010\\ -123.199\\ -27.431\end{bmatrix}$	$\begin{bmatrix}-55.02\\ 88.15\\ -84.4\end{bmatrix}$	$\begin{bmatrix}5.541\\ 13.697\\ 37.041\end{bmatrix}$	$\begin{bmatrix}14.551\\ 21.352\\ 23.678\end{bmatrix}$
4	$\begin{bmatrix}-14.9322\\ -101.133\\ -58.6527\end{bmatrix}$	$\begin{bmatrix}-36.061\\ -114.362\\ -9.045\end{bmatrix}$	$\begin{bmatrix}-62.2\\ 87.16\\ -83.53\end{bmatrix}$	$\begin{bmatrix}21.123\\ 13.229\\ 49.608\end{bmatrix}$	$\begin{bmatrix}47.268\\ 13.973\\ 24.877\end{bmatrix}$
5	$\begin{bmatrix}-21.711\\ -126.540\\ -54.072\end{bmatrix}$	$\begin{bmatrix}-7.262\\ -134.6813\\ -24.6739\end{bmatrix}$	$\begin{bmatrix}-56.7\\ 88.645\\ -84.89\end{bmatrix}$	$\begin{bmatrix}14.450\\ 8.141\\ 29.398\end{bmatrix}$	$\begin{bmatrix}34.990\\ 38.009\\ -30.818\end{bmatrix}$

Table 5.1: Absolute difference between the coordinates of the HJC obtained using ultrasound method and those from both functional and Harrington's predictive methods.

Where gap filling was impossible, some data were cut off since the code requires non-singular matrices constructed from the trajectory data of the markers. This could have introduced error in the results obtained from functional technique. Table 5.1 also compares the results of ultrasound method with those of the Harrington's predictive technique and shows that the latter method gives results that differ considerably. The absolute difference between the locations of HJC derived from the two techniques for each subject is almost consistently greater in the mediolateral and anterior-posterior directions than those obtained while comparing ultrasound technique with the functional technique. The Harrington's technique also appears to give fairly similar for all the subjects.

In order to compare the accuracy of the three techniques, the coordinates of the HJC for subject 3 obtained in Craig, (2011) was used since the subject also participated in the study. It was understood that this may not be a very credible comparison since the locations of subjects' ASISs were not determined by the same person. The assumption was however, that error associated with incorrectly identifying the ASIS would not be large. Table 5.2 shows the comparison.

Ultrasound Result	Harrington's Regression Method	Functional Technique (mm)	MRI Validation (mm)
$\begin{bmatrix} -40.469 \\ -109.502 \\ -64.472 \end{bmatrix}$	$\begin{bmatrix} -55.02 \\ 88.15 \\ -84.4 \end{bmatrix}$	$\begin{bmatrix} -36.010 \\ -123.199 \\ -27.431 \end{bmatrix}$	$\begin{bmatrix} -39.47 \\ -105.53 \\ -22.92 \end{bmatrix}$
$\begin{bmatrix} \Delta x \\ \Delta y \\ \Delta z \end{bmatrix} = \begin{bmatrix} 1.000 \\ 3.972 \\ 41.552 \end{bmatrix}$	$\begin{bmatrix} \Delta x \\ \Delta y \\ \Delta z \end{bmatrix} = \begin{bmatrix} 15.55 \\ 17.38 \\ 61.48 \end{bmatrix}$	$\begin{bmatrix} \Delta x \\ \Delta y \\ \Delta z \end{bmatrix} = \begin{bmatrix} 3.460 \\ 17.669 \\ 4.511 \end{bmatrix}$	

Table 5.2: Absolute differences in the HJC located for subject 3 using MRI and those obtained with the three techniques in current study.

The ultrasound technique located the HJC to within 1mm and 3.972mm of the anterior posterior and medio-lateral coordinates obtained with the MRI respectively. But the difference observed in the inferior-superior direction was much larger. The farthest coordinates obtained using the functional technique was 17.669mm away from the HJC in the medio-lateral direction but the anterior-posterior and superior-inferior axes gave results within 5mm (3.460mm and 4.511mm respectively). The subject's HJC coordinates determined from Harrington's method differed from those estimated from MRI image by over 15mm along all axes.

The results obtained from this study show that the different methods of estimating the HJC have high error tendencies. Using the MRI method as gold standard, the results obtained from the functional technique agree with those of Leardini et al, (1999) in the X and Z directions only. Similarly, the Harrington's method gave results that agree with those of Sangeux et al., (2011) only in the X and Y axes but differ significantly in the Z axis. The ultrasound method developed in this study gave results within the range found by Peters et al., (2010).

Comparing ultrasound results with those of functional and predictive methods, Pietka et al., (2004) observed a discrepancy of 23±6mm and 44 ± 7mm respectively. These findings show that the techniques used in locating the HJC often do so with error. The mislocation error adversely affects the kinetic and kinematic parameters of gait. Stagni et al., (2005) attempted to quantify the effects of HJC mislocation on the dynamic gait parameters of the hip. They showed that the turning moment estimated for the hip joint is in error by up to 22% and 15% when the hip joint centre is respectively mislocated by 30mm anteriorly and 30mm laterally. This large reduction in the hip turning moment would undoubtedly, affect recommendations made based on the outcome of the gait test.

For gait analysis to find widespread application, joint centres must be determined accurately. Hip joint centre in particular, has to be as accurately located as possible since its coordinates are used to determine the femur coordinate system (Plug-in-gait manual) which is used to express dynamic parameters of the knee. This study shows that current techniques of locating the HJC give incorrect results and cannot be applied clinically without extreme caution. However, the ultrasound method has great potential since it actually displays a 2D image of the hip joint. The technique will only require more detailed study to ensure accuracy and to make it more convenient and repeatable. Once these are achieved, the ultrasound method can then be used to define the HJC during robotic total hip or knee arthroplasty and other clinical operations requiring accurate position of the HJC.

CHAPTER 6: CONCLUSION

The hip joint centre is an important biomechanical parameter. It is used to define the point in the hip joint about which the knee moment is calculated. It also plays a key role in defining the thigh- embedded coordinate system in plug in gait model which now has widespread use in many clinics and laboratories. The accuracy with which the hip joint centre is located determines the validity of recommendations based on a gait test.

In recognition of the immense biomechanical importance of the hip joint centre, several techniques were developed for its determination. These techniques, grouped into functional and predictive have undergone many reviews by researchers. However, none of them have found a method devoid of error. Soft tissue artifacts constitute a major challenge in functional techniques which also require the subjects to have substantial hip range of motion. Predictive techniques on the other hand, are usually determined from a special class of people and often locate the hip joint centre with error when used on others. These limitations affect the overall accuracy of the two methods. There was therefore the need to explore the potentials of medical ultrasound in locating the hip joint centre given the current technological advancement of the modern medical ultrasound equipment. This was the motivation behind this study.

Data obtained during subject trial were analysed. The analysis involved derivation of vector equations used to define the pelvic anatomical coordinate system. An anatomical coordinate system was necessary in the present study because it responds to human movements. The Harrington's regression equation and the code used in functional technique both expressed their results in terms of PAC system. Comparison was thus reduced to simple arithmetic.

From the results gathered, the ultrasound method showed consistency with the MRI to within 4mm in medio-lateral and inferior-superior directions suggesting that ultrasound can be used in locating the hip joint centre. The discrepancy observed in the inferior-superior direction however, calls for further investigations in order to fully explore the potentials of modern medical ultrasonography in locating the hip joint centre.

CHAPTER 7: RECOMMENDATIONS

This study requires further investigations to improve results. Improvement in this case was seen as holistic. It was therefore necessary to raise these comments based on the experience gathered in the course of this study

7.1 SPECIAL WEARS FOR SUBJECTS

Scanning a subject's hip joint interferes with the sensitive parts (pubic area) of their body. It was difficult to get subjects due to this requirement. In view of this, special tight wears made with an ultrasound conductor is suggested. Ultrasound scanning of the hip joint can be performed over such materials without loss of resolution.

7.2 SPECIAL PLATFORM

Hip ultrasonography requires the subject to lie supine (*Nestorova,* et al., 2012). The subject feels more comfortable in this position and his femoral head is also exposed from the acetabulum. This therefore has the dual advantage of increasing the subject's comfort and guaranteeing best images of the femoral head. This could not be achieved in the current study because the camera view was obstructed each time it was attempted. A raised platform exposing the two posterior superior iliac spine markers is therefore recommended.

REFERENCES

Abdollah Yousefi, Ergin Tönük, Behzat B. Kentel (2014), In Vivo Verification of Different Hip Joint Center Estimation Methods in Gait Analysis For Healthy Subjects. University of Turkey, 18(SI: Biomechanics), 157-166

Andersen, M. S., Mellon, S., Grammatopoulos, G., & Gill, H. S (2013), Evaluation of the accuracy of three popular regression equations for hip joint centre estimation using computerised tomography measurements for metal-on-metal hip resurfacing arthroplasty patients. Gait & Posture, 38(4), 1044–7, http://doi.org/10.1016/j.gaitpost.2013.01.025

AndriacchiT. P, et al. (1980), A study of lower limb mechanics during stair climbing. Journal of Bone and Joint Surgery, 62-A(1980), pp. 749-757

Backhaus, M, Burmester, G, Gerber, T, Grassi, W, Machold, K, Swen, W, Wakefield, R, Manger, B. (2001), Guidelines for musculoskeletal ultrasound in rheumatology. Annals of the Rheumatic Diseases, 60:641-649. doi:10.1136/ard.60.7.641

Bell, A. L., Brand, R. a., & Pedersen, D. R. (1989), Prediction of hip joint centre location from external landmarks. Human Movement Science, 8(1), 3–16. http://doi.org/10.1016/0167-9457(89)90020-1

Bell, A.L., et al. (1990). J Biomech, 23(6), 617-621

Bouffard Vicky, Begon Mickael Champagne, Payam Farhadnia, Vendittoli Pascal-André, Lavigne Martin, Prince Françoi (2012), Hip joint center localisation: A biomechanical application to hip arthroplasty population. World J Orthop 18; 3(8): 131-136. Available online @ http://www.wjgnet.com/esps/wjo@wjgnet.com

Camomilla V., Cereatti A., Vannozzi G., & Cappozzo A., (2006), An optimized protocol for hip joint centre determination using the functional method. J Biomech 39: 6. 1096-1106

Cappozzo, F. Catani, U. Della Croce, A. Leardini. (1995), Position and orientation of bones during movement: anatomical frame definition and determination. Clinical Biomechanics, 10 pp. 171–178

Davis R.B III, Õunpuu S.,Tyburski, D., Gage J.R. (1991), A gait analysis data collection and reduction technique. Human Movement Science, 10 (1991), pp. 575–587

Eberhart, H.D. and V.T. Inman, (1951), An evaluation of experimental procedures used in a fundamental study of human locomotion. Annals of the New York Academy of Science 15, 1213-1228

Ehrig R.M, Heller M.O, Kratzenstein S, Duda G.N, Trepczynski A, Taylor W.R (2011), The SCoRE residual: A quality index to assess the accuracy of joint estimations".Journal of Biomechanics Vol44, pp. 1400-1404

Gamage S, Lasenby J. (2002), New least squares solutions for estimating the average centre of rotation and axis of rotation. Journal of Biomechanics Vol.35,pp. 87-93.

Harrington, M. et al., (2007), Prediction of the hip joint centre in adults, children and patients with cerebral palsy based on magnetic resonance imaging. Journal of Biomechanics 40 p595-602, 40(3), pp. 595-602.

Hatakeyema T, Uno J, Yamada C., Kishi A., and Hatakeyama H.(2005), "Gel-sol transition of poly(vinyl alcohol) hydrogels formed by freezing and thawing," Thermochimica Acta, vol. 431, no. 1-2, pp. 144–148

Hicks JL and JG Richards (2005), Clinical Applicability of using spherical fitting to find the hip joint centres. Gait and Posture, vol 22, pp138 - 145

Kainz, H., Carty, C. P., Modenese, L., Boyd, R. N., & Lloyd, D. G. (2015). Estimation of the hip joint centre in human motion analysis: A systematic review. Clinical Biomechanics. http://doi.org/10.1016/j.clinbiomech.2015.02.005

Laskin, RX (1984), Alignment of total knee components. Orthopedics 7, 62-72.

Lddr, S., Cf, T. H. I., Rf, H. P. R. F., Mitt, H. F., & Prf, H. (n.d.). Manual of Ma nu al o f diagn ostic ultrasound

Leardini A, Cappozzo A, Catani F, Toksvig-Larsen S, Petitto A, Sforza V, Cassanelli G, Giannini S. (1999), Validation of a functional method for the estimation of hip joint centre location. J Biomech.32:99–103. [PubMed]

Lenaerts, G., Bartels,W., Gelaude, F., Mulier, M., Spaepen, A., Van der Perre, G., Jonkers, I. (2009), Subject-specific hip geometry and hip joint centre location affects calculated contact forces at the hip during gait. J. Biomech. 42 (9), 1246–1251.

Menschik F. (1997), The hip centre as a conchoids shape. J. Biomech 30(9):970-3

Mona Tahvildar-Khazaneh (2013), Locating the hip joint Centre using Ultrasonic Techniques. MSc Thesis,University of Strathclyde, Glasgow

Narouze, S. N. (2011). Atlas of ultrasound-guided procedures in interventional pain management. *Atlas of Ultrasound-Guided Procedures in Interventional Pain Management*, 1–372. http://doi.org/10.1007/978-1-4419-1681-5

O'connor, K. M. O., & Weinhandl, J. T. (n.d.). Hip joint moments using a greater trochanter method of locating the hip joint center. retrieved from http://www.researchgate.net/publication/266504982_hip_joint_moments_using_a_greater_trochanter_method_of_locating_the_hip_joint_center

Peters, A., Baker, R., Morris, M. E., & Sangeux, M. (2012), A comparison of hip joint centre localisation techniques with 3-DUS for clinical gait analysis in children with cerebral palsy. Gait & Posture, 36(2), 282–6. http://doi.org/10.1016/j.gaitpost.2012.03.011

Piazza S.J, Erdemir A, Okita N, Cavanagh P.R.(2004), Assessment of the functional method of hip joint centre location subject to reduced range of hip motion Journal of Biomechanics Vol.34 pp. 349-356

Piętka, E., Kawa, J., & Wieclawek, W. (Eds.). (2014), Information Technologies in Biomedicine, Volume 4 (Vol. 284). Cham: Springer International Publishing. http://doi.org/10.1007/978-3-319-06596-0

Seidel GK, Marchinda DM, Dijkers M, Soutas-Little RW (1995), Hip joint center location from palpable bony landmarks a cadaver study. J Biomech. 28:995–998. [PubMed]

Simpson C., (2011), Predicting the hip joint centre using externally placed markers in gait analysis studies. MSc Thesis University of Strathclyde, Glasgow

Siston, R.A., Delp, S.L. (2006), Evaluation of a new algorithm to determine the hip joint center. J. Biomech. 39 (1), 125–130

Siwach R. C. and Dahiya S.(2003), Anthropometric study of proximal femur and its clinical application. Indian Journal of Orthop vol 37, issue4: 247-251

Stagni R, Fantozzi S, Cappello A, Leardini A (2005), "Quantification of soft tissue artefact in motion analysis by combining 3D fluoroscopy and stereophotogrammetry: a study on two subjects". Clinical Biomechanics Vol20 pp. 320-329

Tylkowski, C.M., Simon, S.R., Mansour, J.M., (1982), Internal rotation gait in spastic cerebral palsy in the hip. Proceedings of the 10th Open Scientific Meeting of the Hip Society. Mosby, St. Louis, pp. 89–125.

Yoshioka, Y., Siu, D., & Cooke, T. D. (1987). The anatomy and functional axes of the femur. The Journal of Bone and Joint Surgery. American Volume, 69(6), 873–80. Retrieved from http://www.ncbi.nlm.nih.gov/pubmed/3597501

Nestorova, R., Vlad, V., Petranova, T., Porta, F., Radunovic, G., Micu, M. C., & Iagnocco, A. (2012). Ultrasonography of the hip. Medical Ultrasonography, 14(3), 217–224. http://doi.org/10.1016/j.cult.2012.08.002

Diagnostic Ultrasound Safety: A summary of the technical report "Exposure Criteria for Medical Diagnostic Ultrasound: II. Criteria based on all Known Mechanisms" issued by the National Council on Radiation Protection and Measurements. Available at: htttp://www.ncrponline.org/Publications/Reports/Misc_PDFs/Ultrasound%20Summary--NCRP.pdf

Optical Motion Capture. Retrieved from :http://mocap.csit.carleton.ca/index.php?Section=ViconIQ&Item=Tabs&Page=Calibration

Wynn Kapit, Lawrence M Elson (2002), The Anatomy Colouring Bookb 3rd ed. Benjamin Cummings

Running head: The Role Of Ultrasound In Orthopedics (2012), A Review OF The Role of Ultrasound in Orthopedics: A Review of the Literature .November 13, 2012. (2012), 1–15.

Plug in gait manual.(From http://wweb.uta.edu/faculty/ricard/Classes/KINE-5350/PIGManualver1.pdf)

Web Images

(https:// http://free-stock-illustration.com/hip+muscles+anatomy?image=1262775607

http://www.rudyard.org/hip-joint-anatomy/)

http://www.rudyard.org/hip-joint-anatomy

https:// http://free-stock-illustration.com/hip+muscles+anatomy?image=1262775607

http://nick-carrington.co.uk/uploads/images/hip-anatomy.jpg

APPENDIX A

```
%MATLAB code used to visualize the circle representing the head of
femur and its offset from
%the origin of the probe reference frame.
% The offset is to be added to the calculation of xm


%Input an n x 2 matrix of points to be fitted with circle
XY = input(' 1 x 2 matrix of n discretized points on the femoral head :
');


Par = CircleFitByPratt(XY);% Fitting the circle according to Pratt
method

points = XY;
disp(points)
t = linspace(0, 2 * pi);

p = Par(1,2) + Par(1,3) * sin(t);

q = Par(1,1) + Par(1,3) * cos(t);

figure;
plot(q,p,'r');

axis equal;

hold on

disp('radius of best fit circle is :'); disp(Par(1,3));

disp('offset from probe centre line (to be added or subtracted
accordingly) is:');
disp(Par(1,1));

disp('The distance from the probe tip to the centre of fitted circle
''b'', is:');
disp(Par(1,2));

m = linspace(0,Par(1,2));


plot(Par(1,1),m,'b');

hold off;
```

```
Function Par = CircleFitByPratt(XY)

%------------------------------------------------------------------------
----
%
%     Circle fit by Pratt
%      V. Pratt, "Direct least-squares fitting of algebraic surfaces",
%      Computer Graphics, Vol. 21, pages 145-152 (1987)
%
%     Input:  XY(n,2) is the array of coordinates of n points
x(i)=XY(i,1), y(i)=XY(i,2)
%
%     Output: Par = [a b R] is the fitting circle:
%                           center (a,b) and radius R
%
%     Note: this fit does not use built-in matrix functions (except
"mean"),
%           so it can be easily programmed in any programming language
%
%------------------------------------------------------------------------
----

n = size(XY,1);      % number of data points

centroid = mean(XY);   % the centroid of the data set

%     computing moments (note: all moments will be normed, i.e. divided
by n)

Mxx=0; Myy=0; Mxy=0; Mxz=0; Myz=0; Mzz=0;

for i=1:n
    Xi = XY(i,1) - centroid(1);  %  centering data
    Yi = XY(i,2) - centroid(2);  %  centering data
    Zi = Xi*Xi + Yi*Yi;
    Mxy = Mxy + Xi*Yi;
    Mxx = Mxx + Xi*Xi;
    Myy = Myy + Yi*Yi;
    Mxz = Mxz + Xi*Zi;
    Myz = Myz + Yi*Zi;
    Mzz = Mzz + Zi*Zi;
end

Mxx = Mxx/n;
Myy = Myy/n;
Mxy = Mxy/n;
Mxz = Mxz/n;
Myz = Myz/n;
Mzz = Mzz/n;

%    computing the coefficients of the characteristic polynomial
```

```
Mz = Mxx + Myy;
Cov_xy = Mxx*Myy - Mxy*Mxy;
Mxz2 = Mxz*Mxz;
Myz2 = Myz*Myz;

A2 = 4*Cov_xy - 3*Mz*Mz - Mzz;
A1 = Mzz*Mz + 4*Cov_xy*Mz - Mxz2 - Myz2 - Mz*Mz*Mz;
A0 = Mxz2*Myy + Myz2*Mxx - Mzz*Cov_xy - 2*Mxz*Myz*Mxy + Mz*Mz*Cov_xy;
A22 = A2 + A2;

epsilon=1e-12;
ynew=1e+20;
IterMax=20;
xnew = 0;

%    Newton's method starting at x=0

for iter=1:IterMax
    yold = ynew;
    ynew = A0 + xnew*(A1 + xnew*(A2 + 4.*xnew*xnew));
    if (abs(ynew)>abs(yold))
        disp('Newton-Pratt goes wrong direction: |ynew| > |yold|');
        xnew = 0;
        break;
    end
    Dy = A1 + xnew*(A22 + 16*xnew*xnew);
    xold = xnew;
    xnew = xold - ynew/Dy;
    if (abs((xnew-xold)/xnew) < epsilon), break, end
    if (iter >= IterMax)
        disp('Newton-Pratt will not converge');
        xnew = 0;
    end
    if (xnew<0.)
        fprintf(1,'Newton-Pratt negative root:  x=%f\n',xnew);
        xnew = 0;
    end
end

%    computing the circle parameters

DET = xnew*xnew - xnew*Mz + Cov_xy;
Center = [Mxz*(Myy-xnew)-Myz*Mxy , Myz*(Mxx-xnew)-Mxz*Mxy]/DET/2;

Par = [Center+centroid , sqrt(Center*Center'+Mz+2*xnew)];

k = sqrt(Center*Center'+Mz+2*xnew)

end    %    CircleFitByPratt
```

APPENDIX B

```
%PROGRAMME to determine the coordinates of the Hip Joint Centre in
global
%reference frame.

%By Eze Solomon Chika

% Inputs to coordinate points must be in the form of 1x3 matrices

P = input('Enter the coordinates of point 1 : ');% coordinates of the
probe marker 1

Q = input('Enter the coordinates of point 2 : ');% coordinates of the
probe marker 2
%
%
R = input('Enter the coordinates of point 3 : ');% coordinates of the
probe marker 3

%
b = input('Enter the value of b : ');
%

N = [(P(1,1)+ R(1,1))/2 (P(1,2)+ R(1,2))/2 (P(1,3)+ R(1,3))/2];

disp('Probe midpoint coordinate is:'); N

%%
%Calculating the coordinates of the HJC in global reference frame by
%interpolation

% The geometry forms two similar triangles
%HJC coordinates are calculated by interpolation

xc = Q(1,1) - ((Q(1,1) - N(1,1)) * (b + 77.68)) / 77.68;

yc = Q(1,2) - ((Q(1,2) - N(1,2)) * (b + 77.68)) / 77.68;

zc = Q(1,3) - ((Q(1,3) - N(1,3)) * (b + 77.68)) / 77.68;


disp('Coordinates of the HJC in global reference frame is :');


disp([xc yc zc]);

%Computing the location of the HJC using ASIS as origin
```

```
A = input('Enter the coordinates of the ASIS : ');

x = -A(1,1) + xc; y = -A(1,2) + yc; z = -A(1,3) + zc;

disp('And the coordinates of the HJC with respect to the ASIS is:');

%Display the coordinates of the HJC in Cartesian coordinate frame of
the
%laboratory

disp(x);

disp(y)

disp(z);
```

APPENDIX C

```
%Programme to transform the HJC from the laboratoy GRF to ACS.
% GRF = Ground reference frame
% ACS = Pelvic anatomical coordinate system

% By Eze Solomon Chika

RASIS = input('Please enter the coordinates of the RASIS: ');% 1 x 3
matrix

LASIS = input('Please enter the coordinates of the LASIS:  ');% 1 x 3
matrix

HJC = input('Please enter the coordinates of the HJC:  ');% 1 x 3
matrix

y = RASIS - LASIS; %calculates the inter ASIS distance

v1 = y/norm(y); % computes the unit vector in anatomical Y axis. This
is known as e paY


PSISs = input(' enter the coordinates of the two PSISs; in 2 x 3
matrix:  ');

%Compute the midpoints of PSISs

PSIS = [(PSISs(1,1) + PSISs(2,1))/2 (PSISs(1,2) + PSISs(2,2))/2,
(PSISs(1,3) + PSISs(2,3))/2]


x =      PSIS - RASIS ; % computes the x components

x1 = cross(x,v1); %Computes the cross product of the two vectors

v2 = x1/norm(x1);% unit vector in x direction

v3 = cross(v1,v2);  % computes the third orthogonal axis

ePa = [v1 v2 v3]


HJC_disp = HJC - (RASIS + LASIS)/2;% Displacement of the HJC from the
midpoint of inter ASIS span

%Compute the coordinates of the HJC in PAC system
HJC_coord_x = dot(v3,HJC_disp);

HJC_coord_y = dot(v1,HJC_disp);
```

```
HJC_coord_z = dot(v2,HJC_disp);

Hip_joint = [HJC_coord_x HJC_coord_y HJC_coord_z]
```

APPENDIX D

Linda Gilmour

From:	Linda Gilmour
Sent:	16 June 2015 11:52
To:	Stephanos Solomonidis
Cc:	'solomon.eze.2014@uni.strath.ac.uk'
Subject:	Approval for Paper DEC.BioMed.2015.58
Attachments:	E mail encouraging subjects to participate.docx

Thank you for the above revised ethics application.

The Departmental Ethics Committee is satisfied with all changes in the revised application but asked that you **use the attached recruitment e-mail** which they have amended and gave their approval for this project with immediate effect.

Good luck with your project and remember you must inform us in writing of any changes to the project and any unforeseen circumstances which arise during the project.

Regards

Linda Gilmour *(Secretary to)*
Departmental Ethics Committee

Regards

Linda Gilmour

Secretary to Professor Terry Gourlay
Department of Biomedical Engineering
University of Strathclyde
Wolfson Centre
106 Rottenrow East
Glasgow G4 0NW
linda.gilmour@strath.ac.uk
Tel: (+44) 141 548 3298
Fax: (+44) 141 552 6098
http://www.strath.ac.uk/biomedeng